Electronic Supplementary Material (ESI) for New Journal of Chemistry.

Electronic Supplementary Information

Table of contents

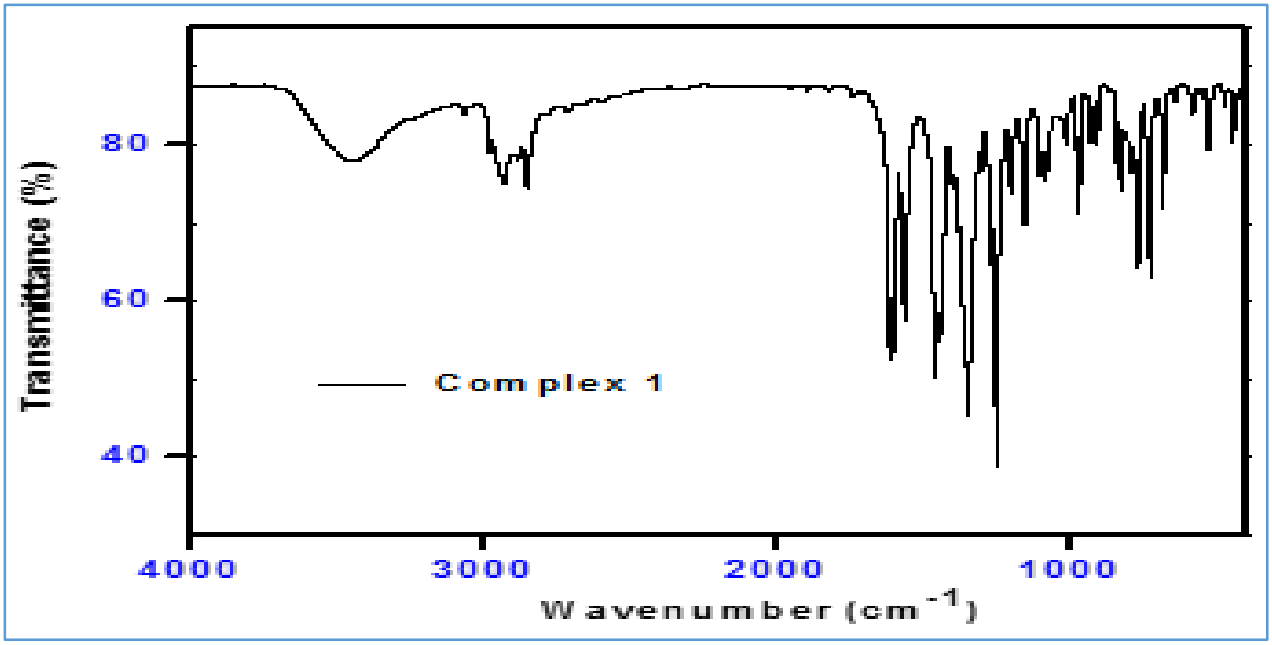

Figure S1: FT-IR spectrum of complex **1.**

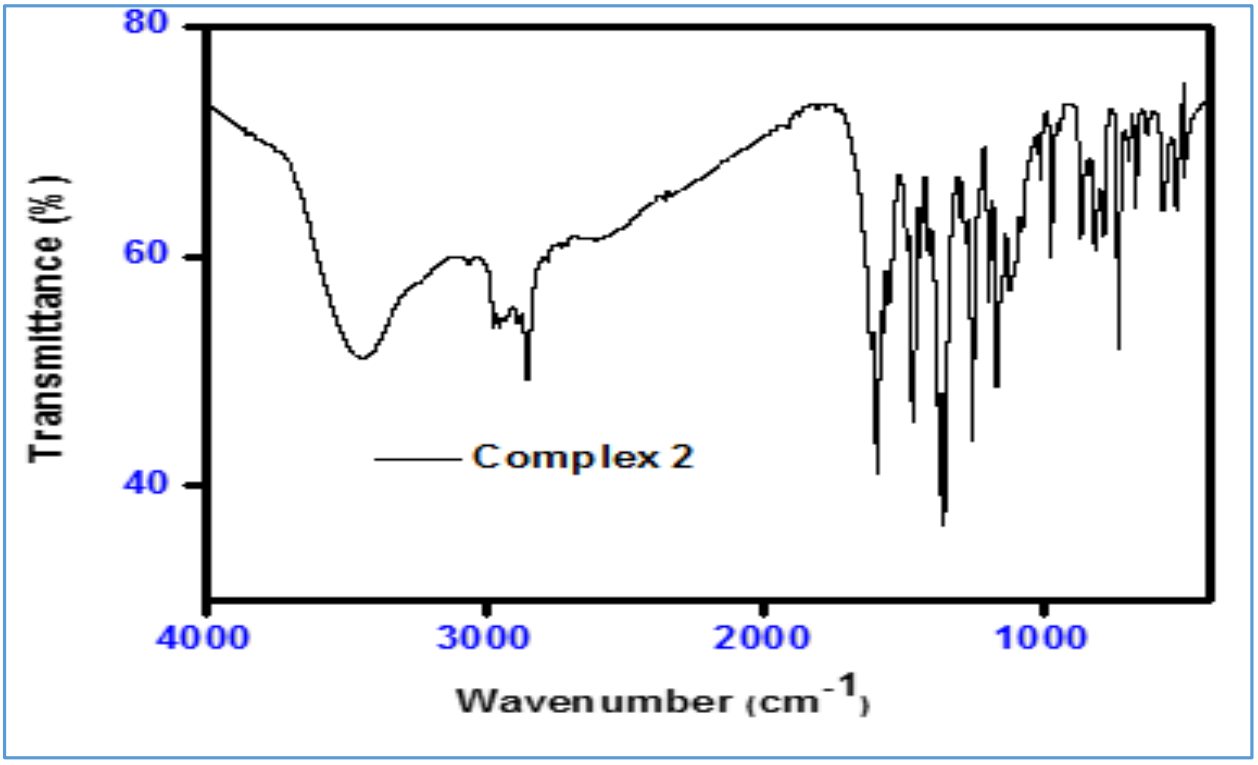

Figure S2: FT-IR spectrum of complex **2**

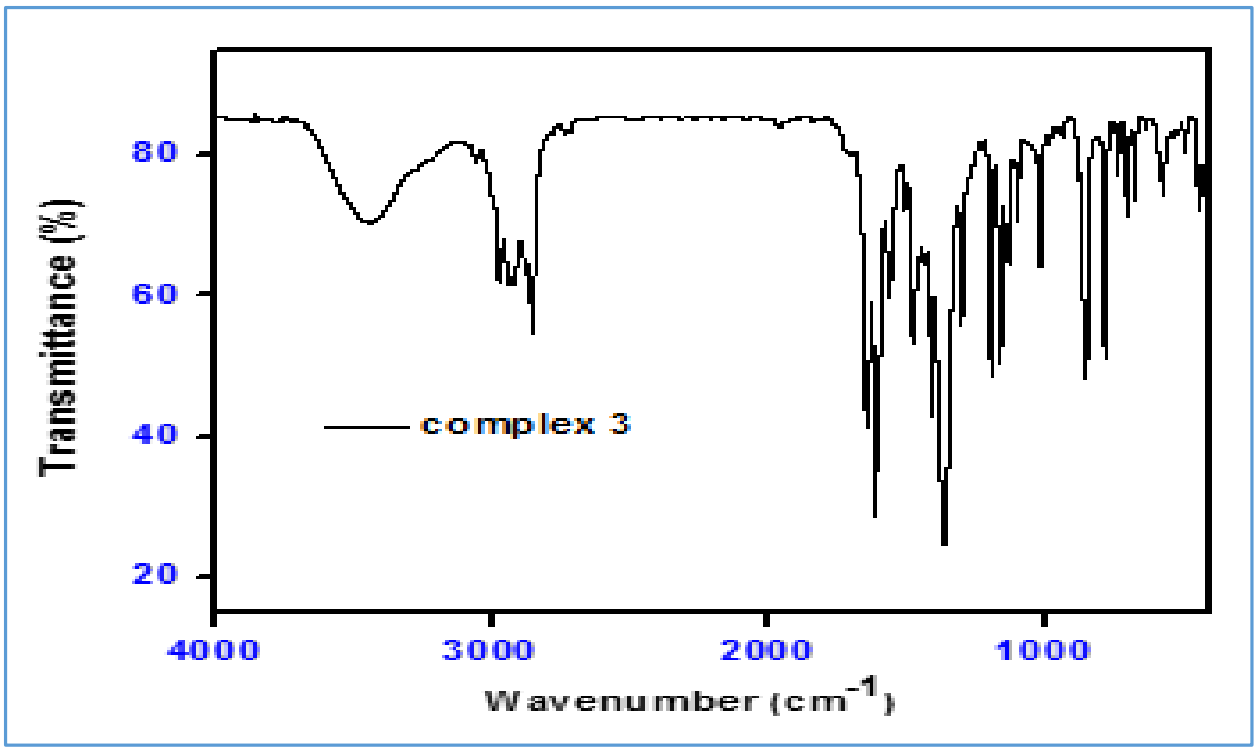

Figure S3: FT-IR spectrum of complex **3**.

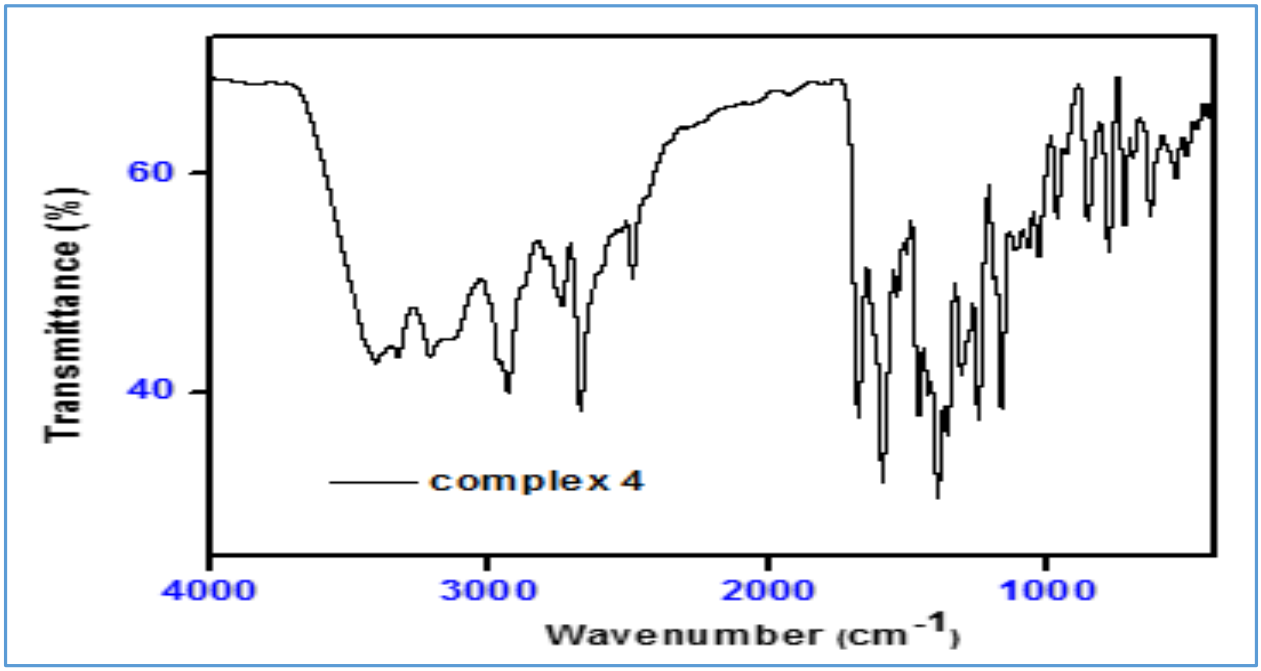

Figure S4: FT-IR spectrum of complex **4**.

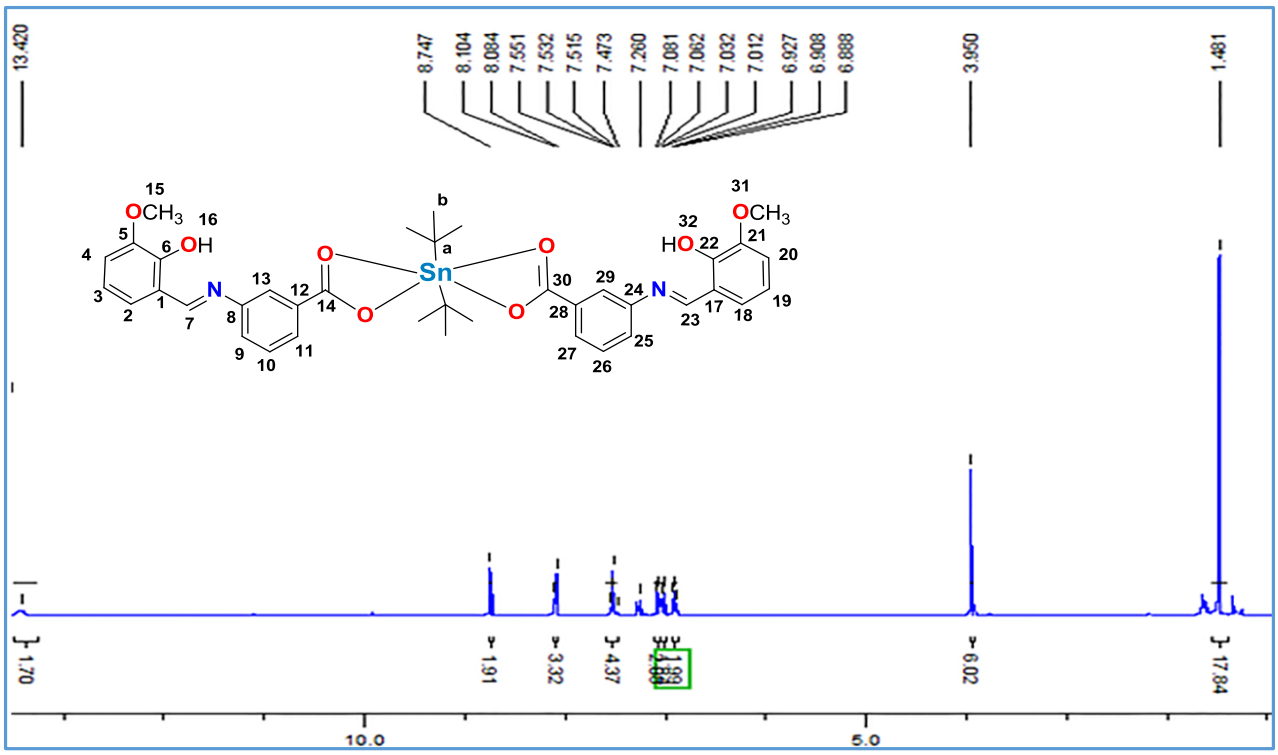

Figure S5: ^{1}H NMR spectrum of complex **1** recorded in $CDCl_3$.

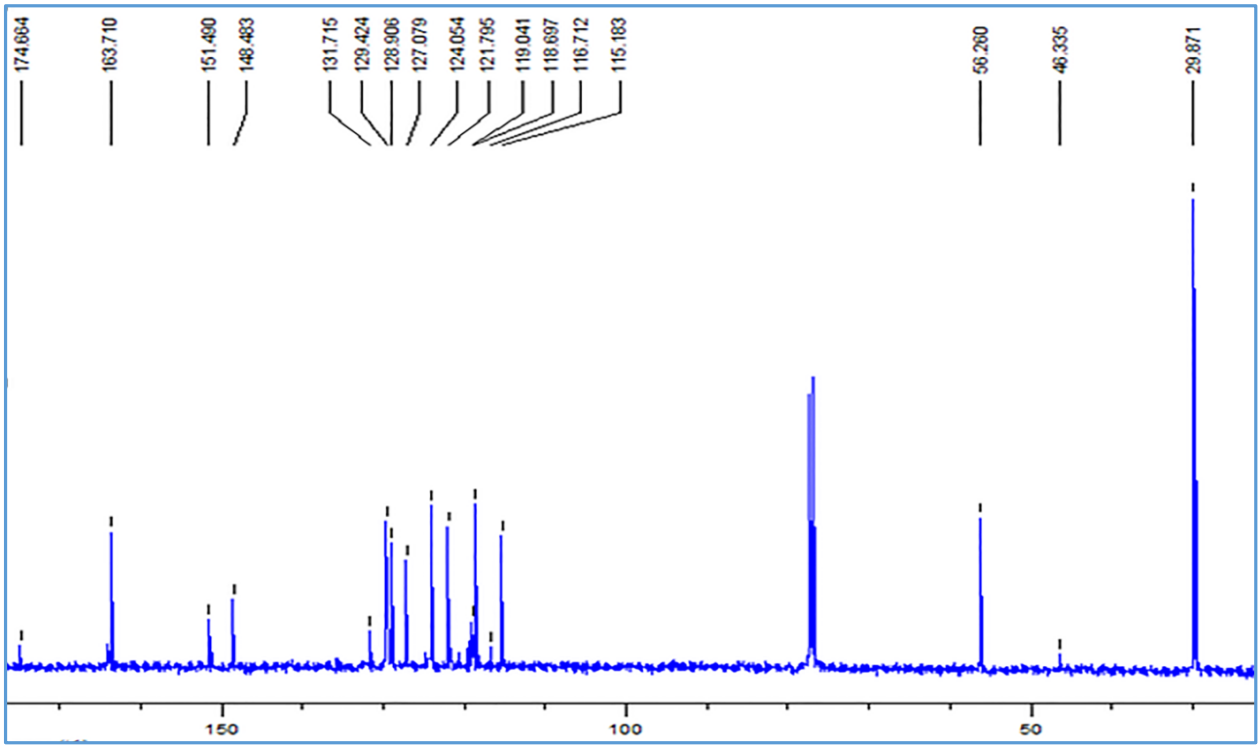

Figure S6: $^{13}C\{^{1}H\}$ NMR spectrum of complex **1** recorded in $CDCl_3$.

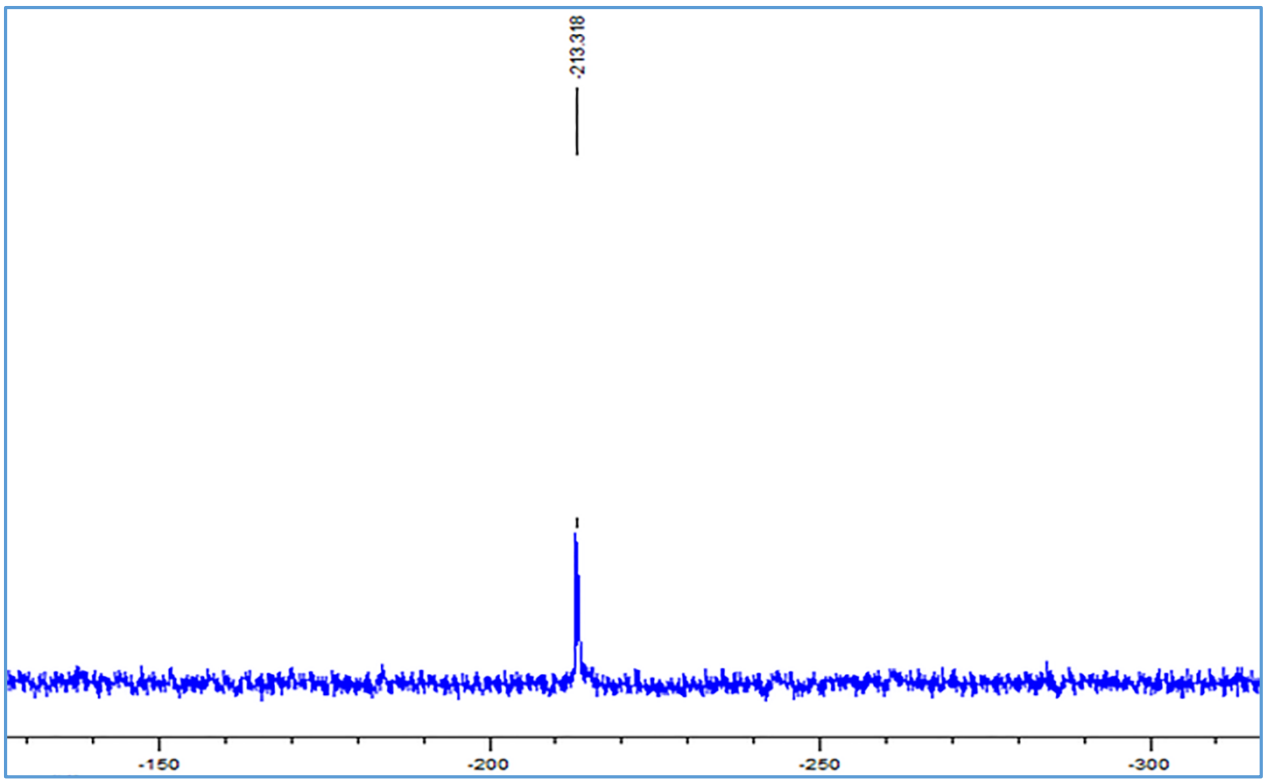

Figure S7: ^{119}Sn NMR spectrum of complex **1** recorded in $CDCl_3$

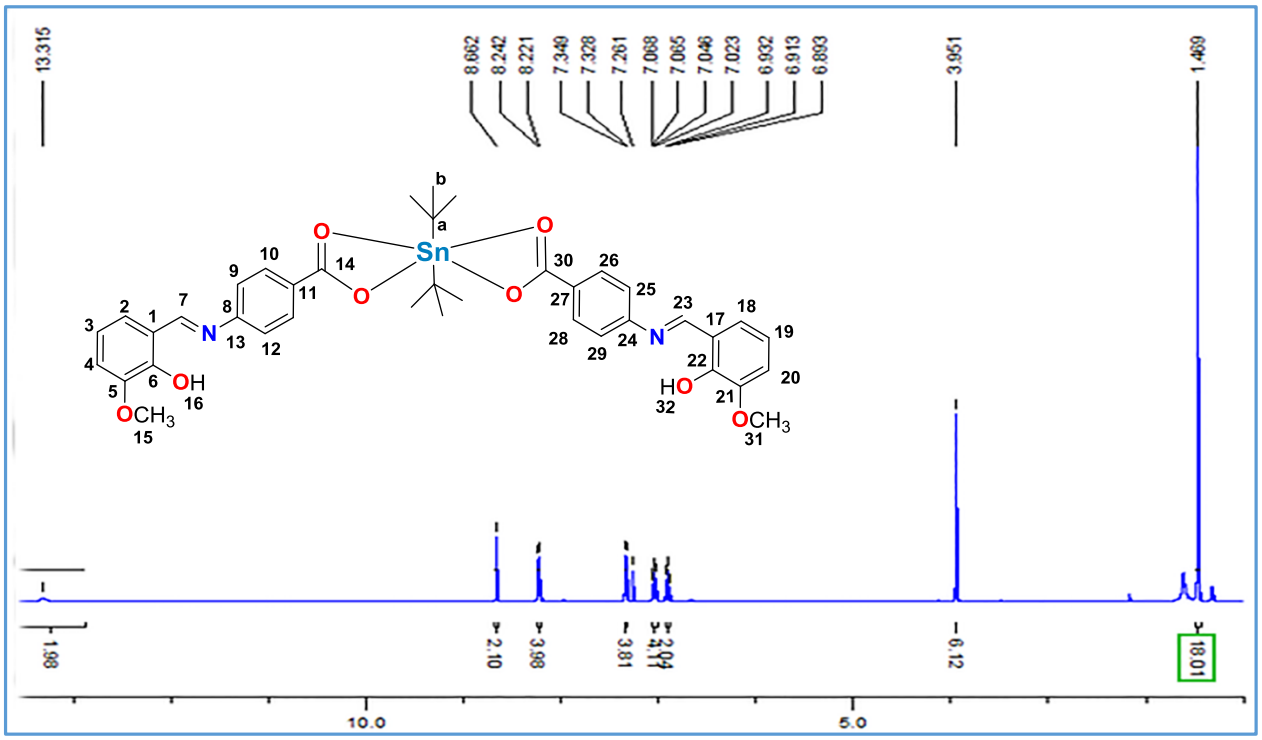

Figure S8: ^{1}H NMR spectrum of complex **2** recorded in $CDCl_3$.

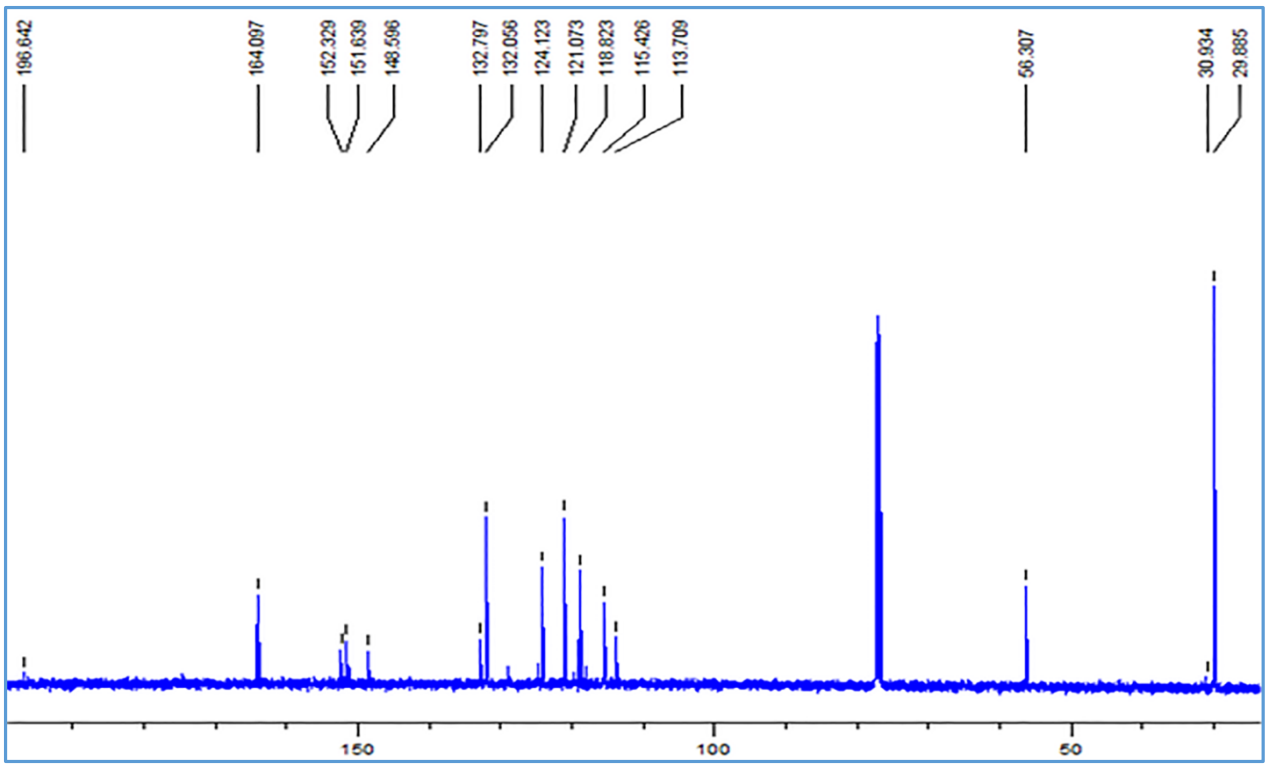

Figure S9: $^{13}C\{^{1}H\}$ NMR spectrum of complex **2** recorded in $CDCl_3$.

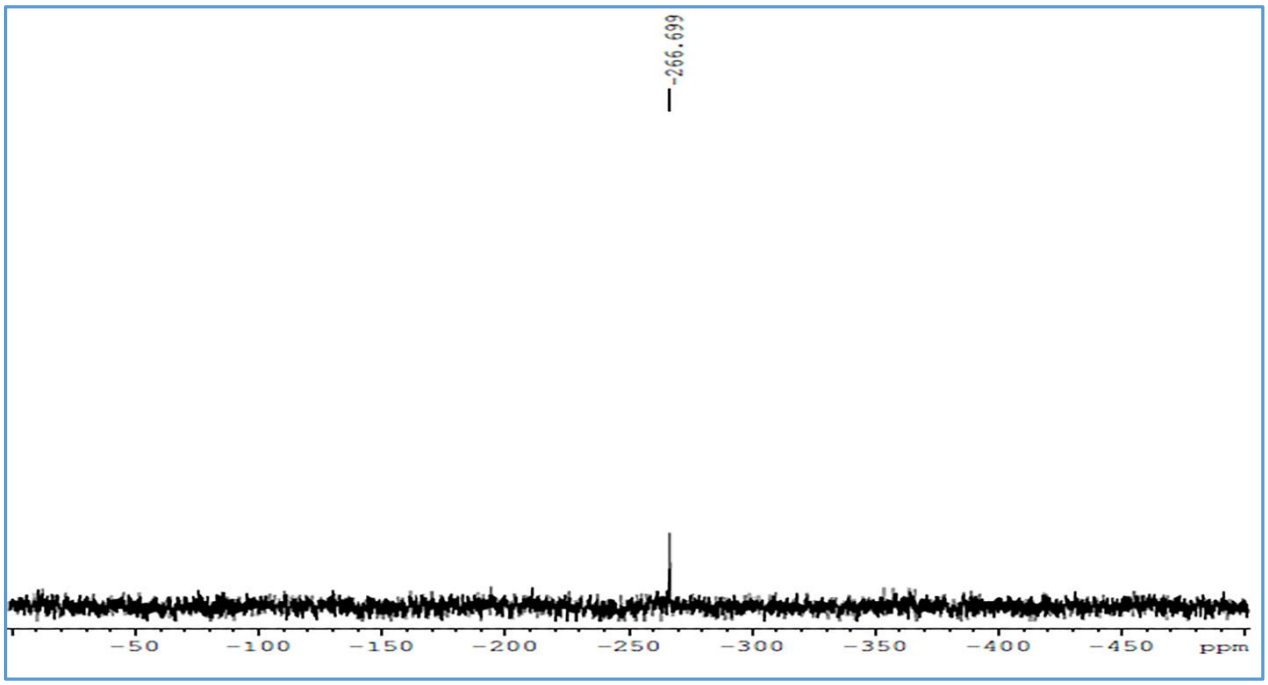

Figure S10: ^{119}Sn NMR spectrum of complex **2** recorded in $CDCl_3$.

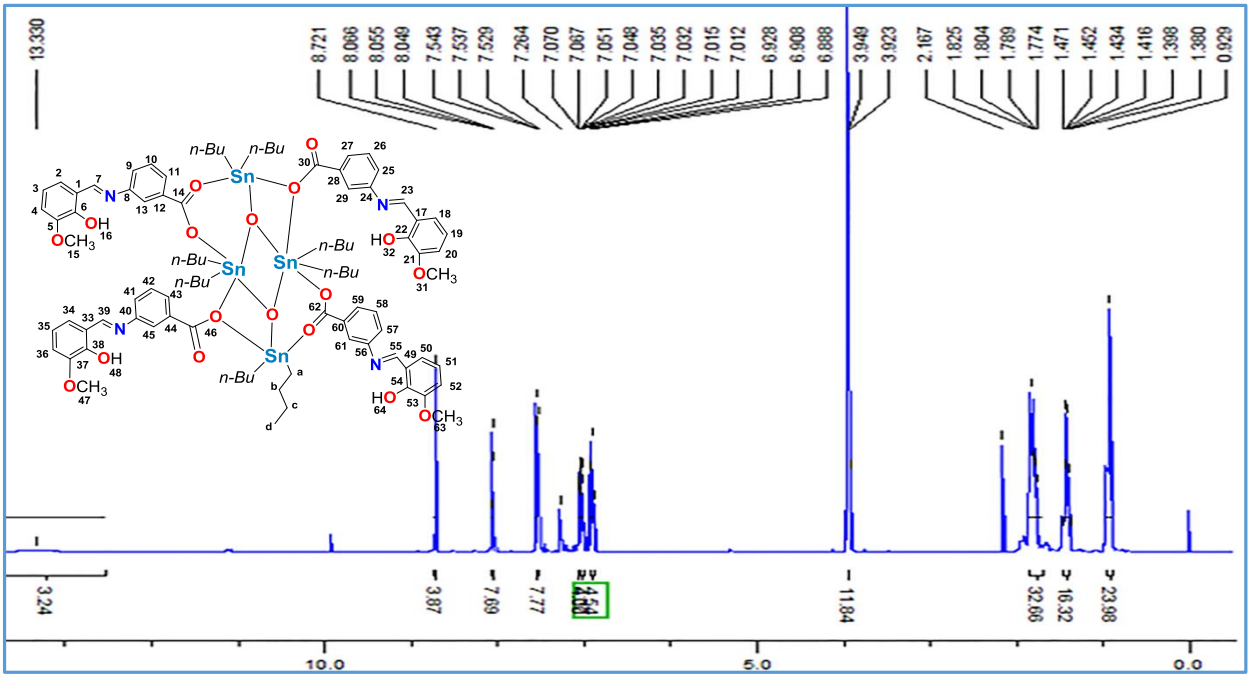

Figure S11: ^{1}H NMR spectrum of complex **3** recorded in $CDCl_3$.

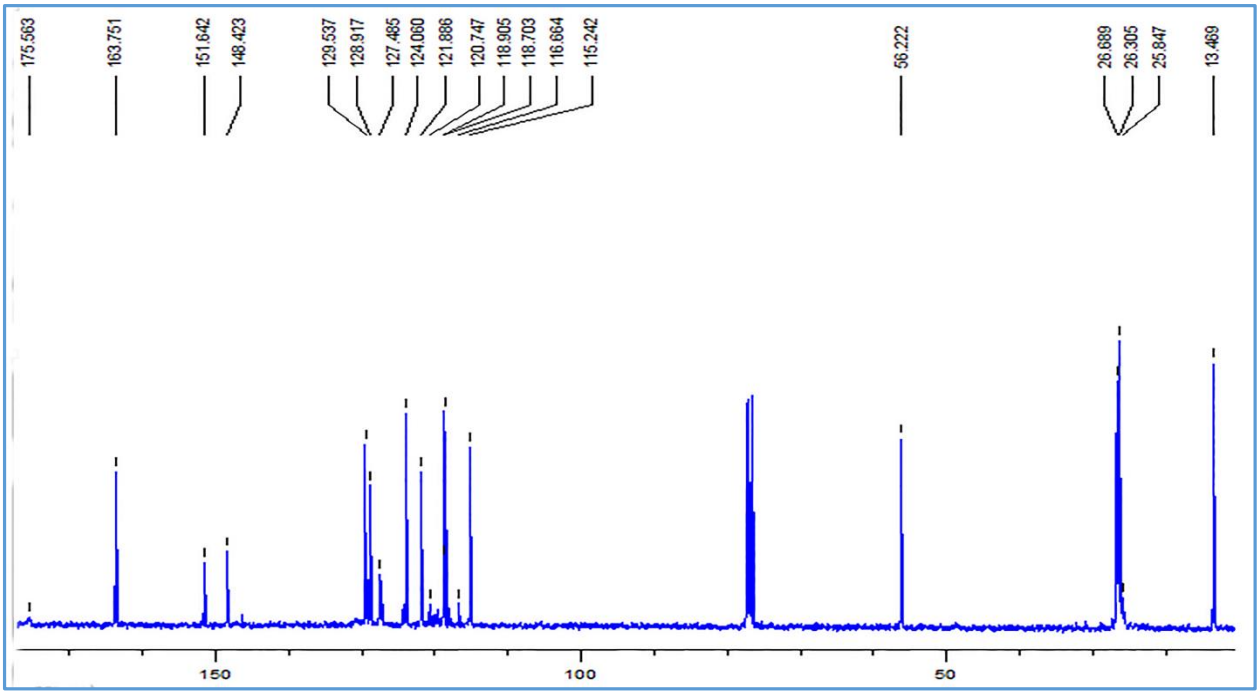

Figure S12: $^{13}C\{^{1}H\}$ NMR spectrum of complex **3** recorded in $CDCl_3$.

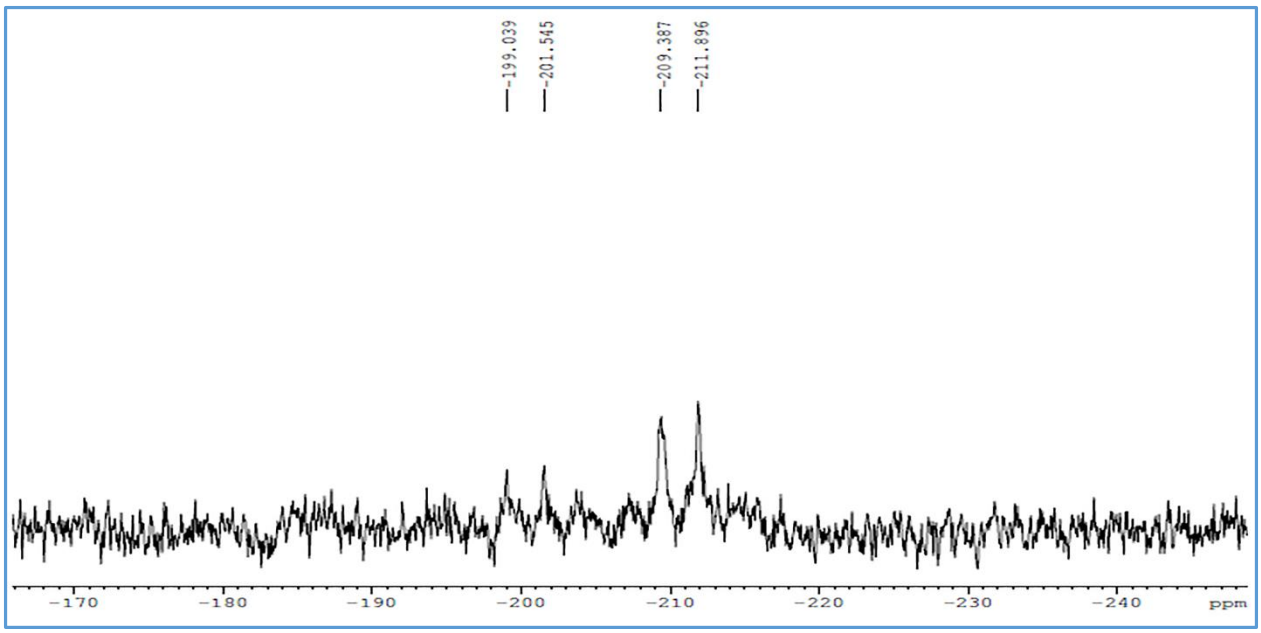

Figure S13: ^{119}Sn NMR spectrum of complex **3** recorded in $CDCl_3$

.

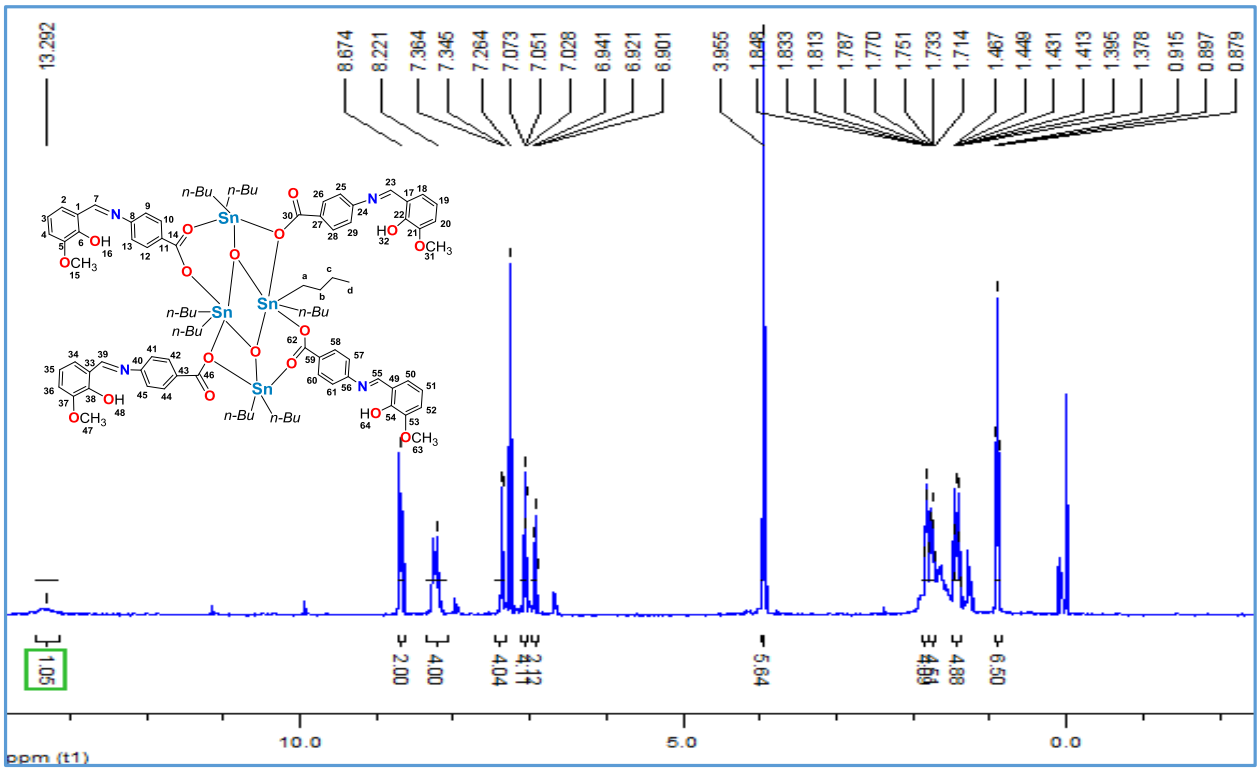

Figure S14: ^{1}H NMR spectrum of complex **4** recorded in $CDCl_3$.

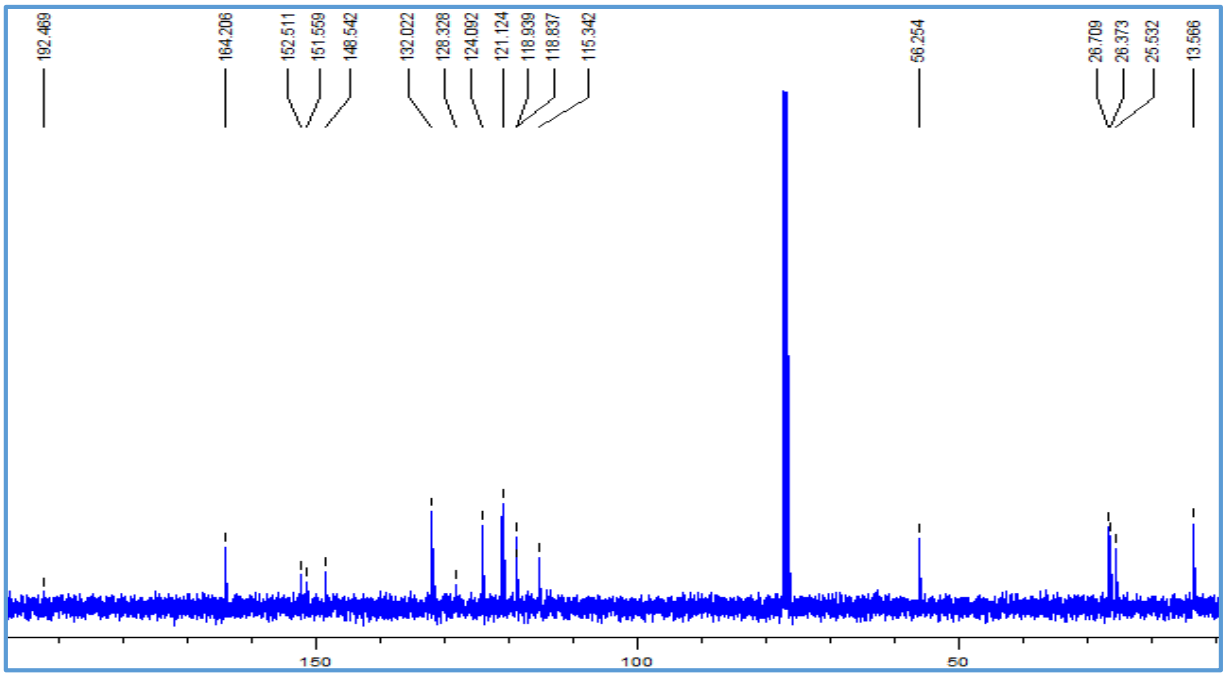

Figure S15: $^{13}C\{^{1}H\}$ NMR spectrum of complex **4** recorded in $CDCl_3$.

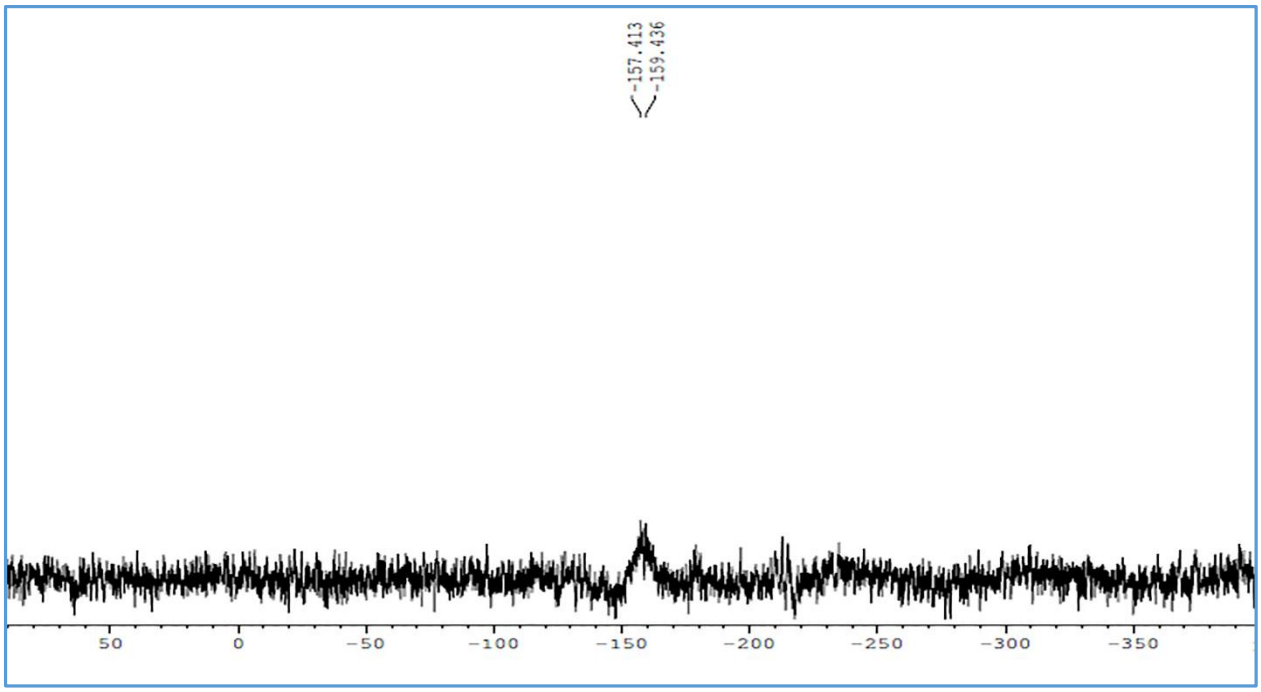

Figure S16: ^{119}Sn NMR spectrum of complex **4** recorded in $CDCl_3$

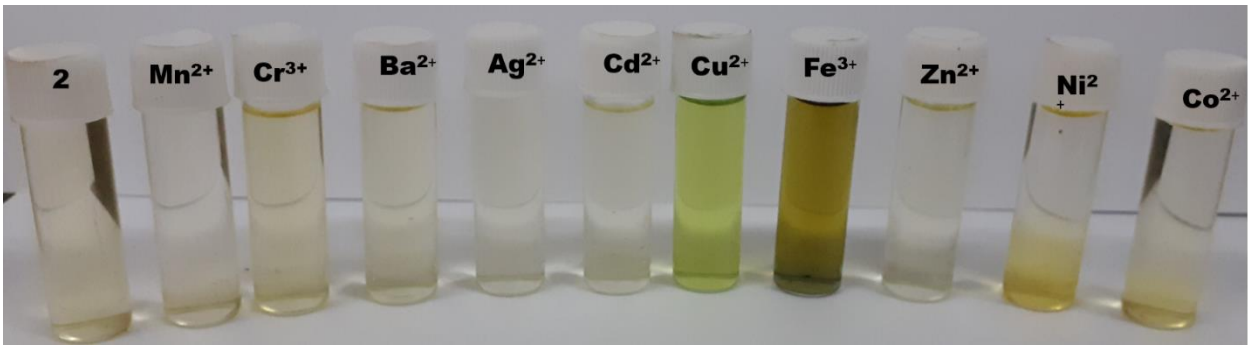

Figure S17: Naked-eye color changes observed due to the addition of equivalent amounts of metal salts in complex **2**.

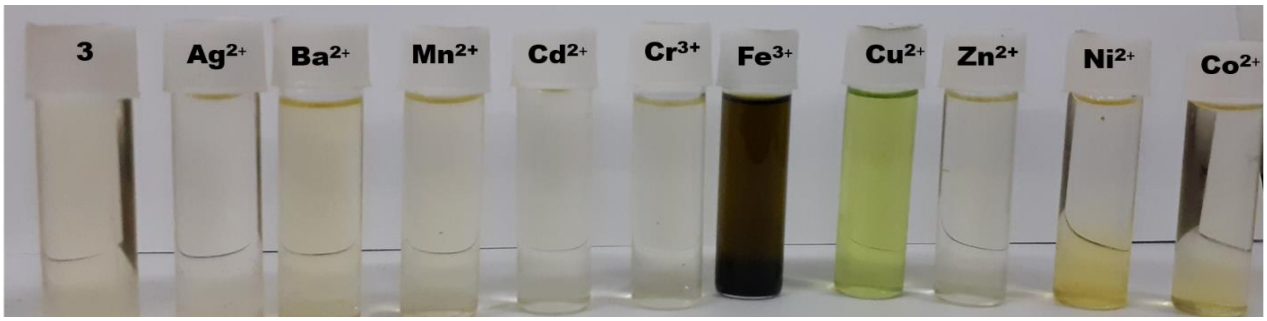

Figure S18: Naked-eye color changes observed due to the addition of equivalent amounts of metal salts in complex **3**.

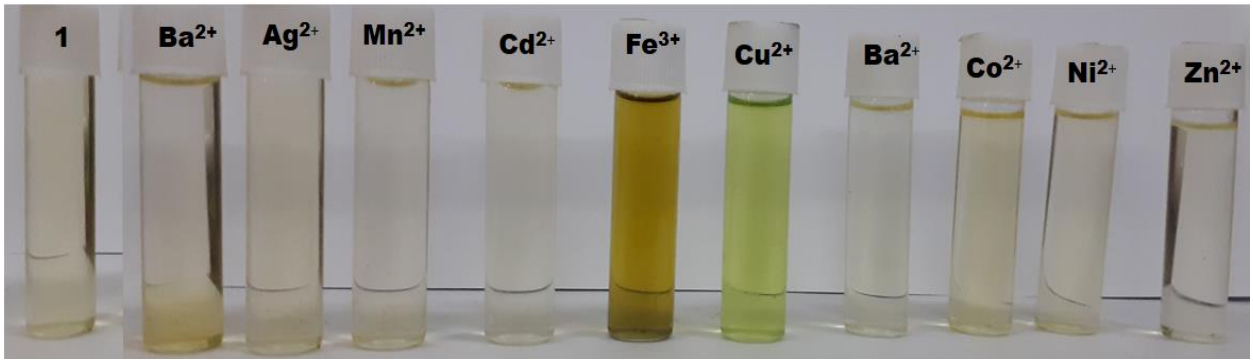

Figure S19: Naked-eye color changes observed due to the addition of equivalent amounts of metal salts in complex **4**

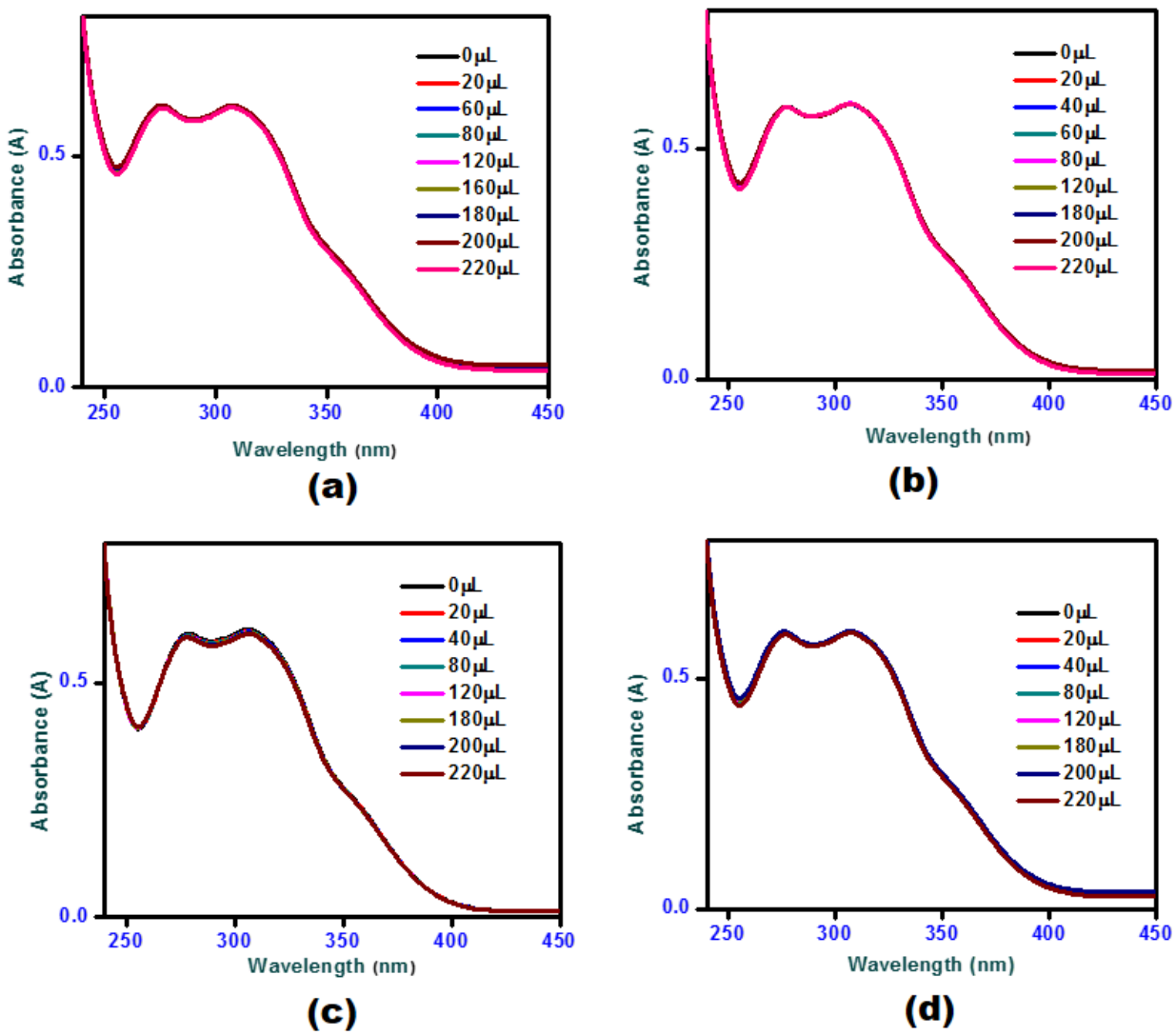

Figure S20: Absorption spectral variation of complex **1** (2 x 10^{-5} mol dm^{-3}) with the addition of 1-5 equivalent of nitrate salts (2 x 10^{-4} mol dm^{-3}) of **(a)** Ag^{+} **(b)** Ba^{2+} **(c)** Cd^{2+} **(d)** Co^{2+}in DCM-methanol (1:9).

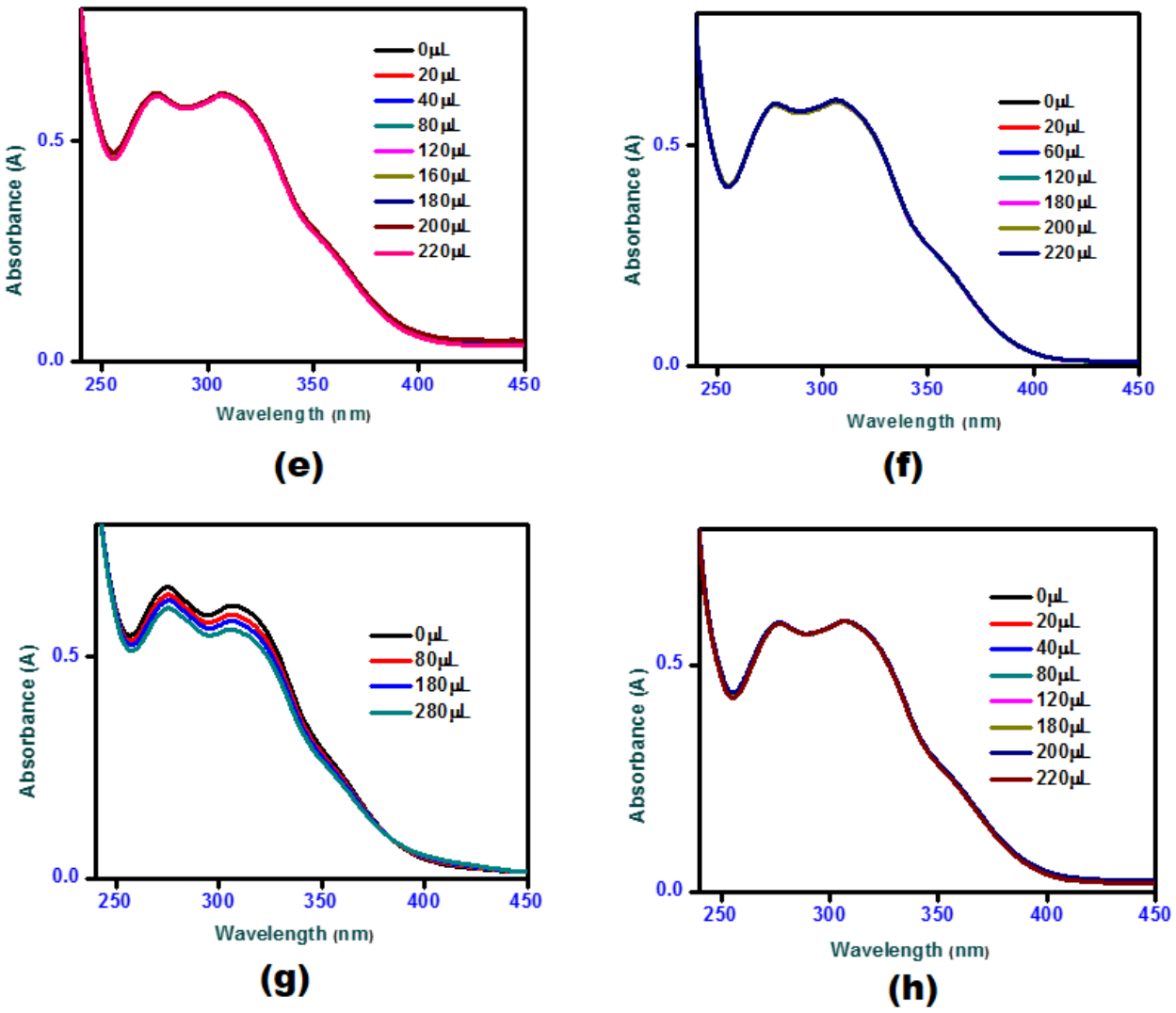

Figure S21: Absorption spectral variation of complex **1** (2 x 10^{-5} mol dm^{-3}) with the addition of 1-5 equivalent of nitrate salts (2 x 10^{-4} mol dm^{-3}) of **(e)** Cr^{3+} **(f)** Mn^{2+} **(g)** Ni^{2+} **(h)** Zn^{2+}in DCM-methanol (1:9).

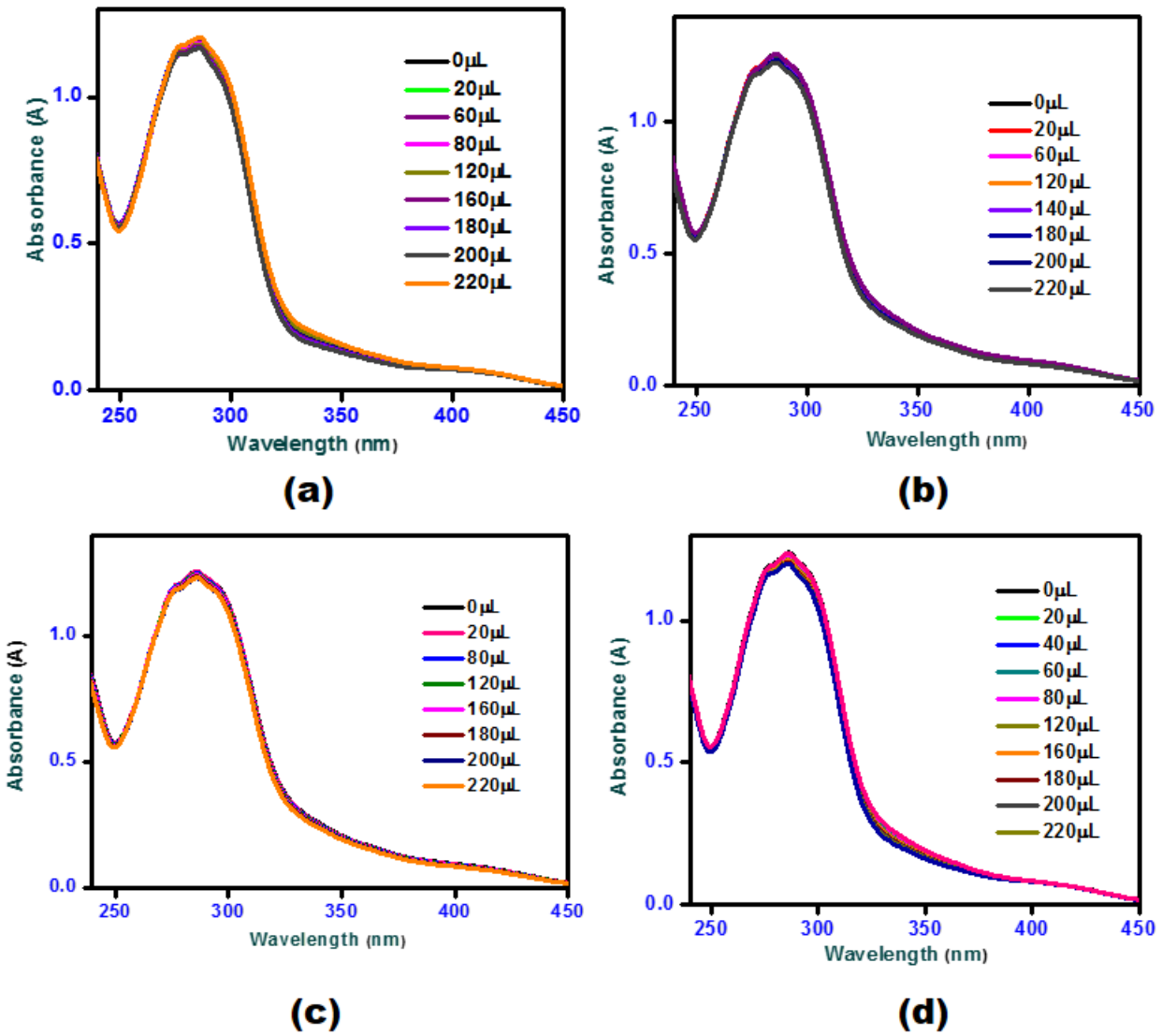

Figure S22: Absorption spectral variation of complex **2** (2 x 10^{-5} mol dm^{-3}) with the addition of 1-5 equivalent of nitrate salts (2 x 10^{-4} mol dm^{-3}) of **(a)** Ag^{+} **(b)** Ba^{2+} **(c)** Cd^{2+} **(d)** Co^{2+}in DCM-methanol (1:9).

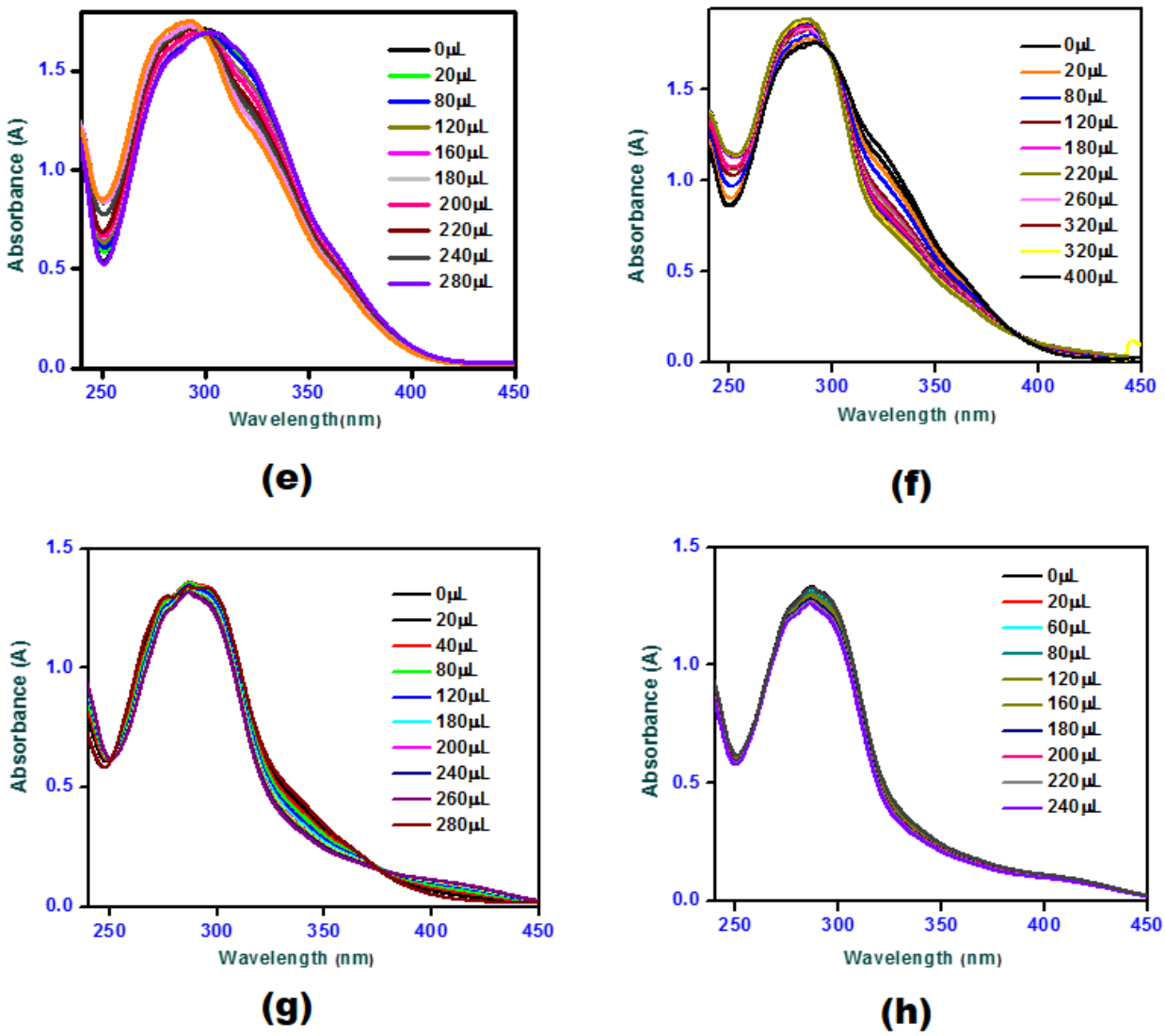

Figure S23: Absorption spectral variation of complex **2** (2 x 10^{-5} mol dm^{-3}) with the addition of 1-5 equivalent of nitrate salts (2 x 10^{-4} mol dm^{-3}) of **(e)** Cr^{3+} **(f)** Mn^{2+} **(g)** Ni^{2+} **(h)** Zn^{2+}in DCM-methanol (1:9).

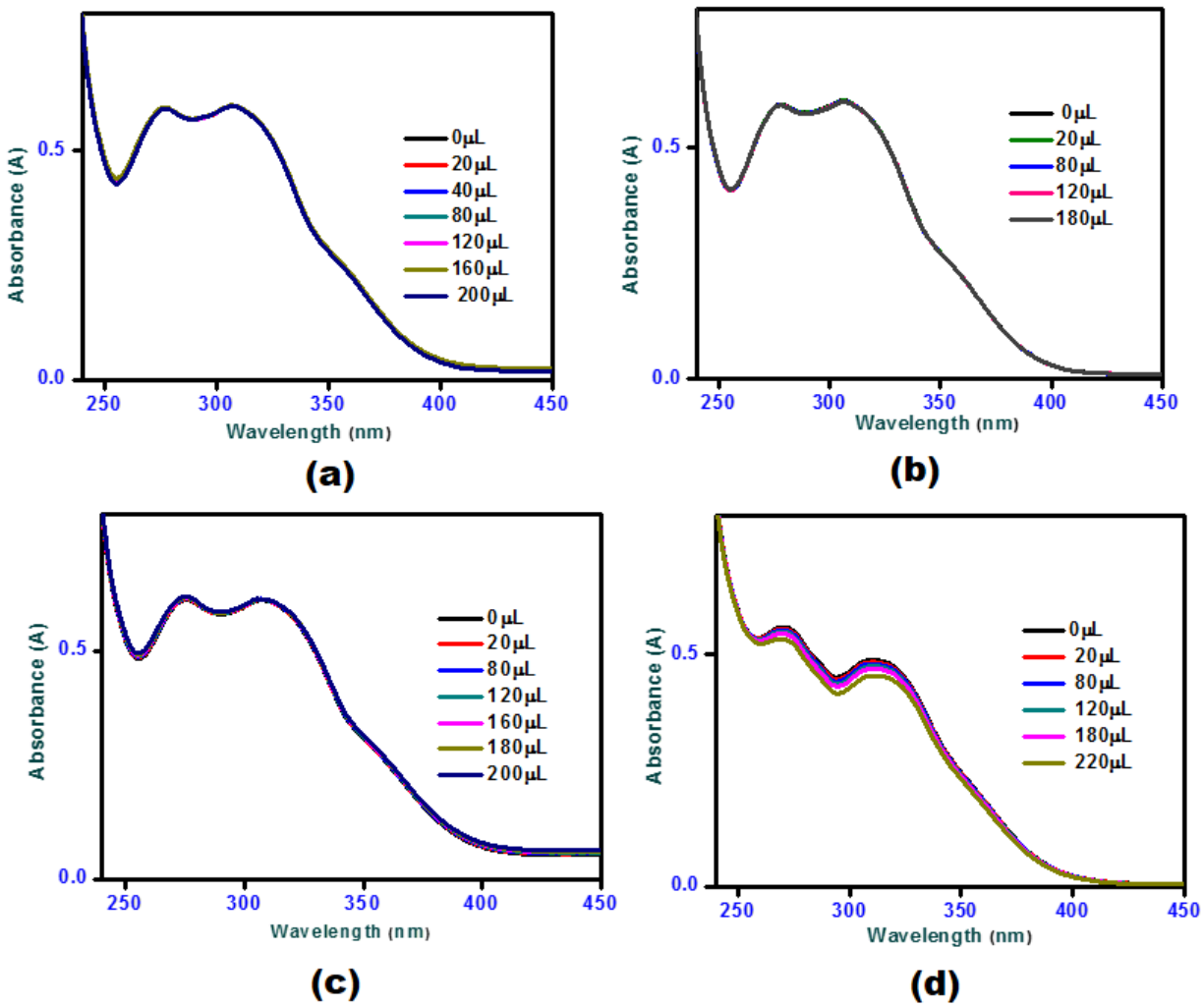

Figure S24: Absorption spectral variation of complex **3** (2 x 10^{-5} mol dm^{-3}) with the addition of 1-5 equivalent of nitrate salts (2 x 10^{-4} mol dm^{-3}) of **(a)** Ag^{+} **(b)** Ba^{2+} **(c)** Cd^{2+} **(d)** Co^{2+}in DCM-methanol(1:9).

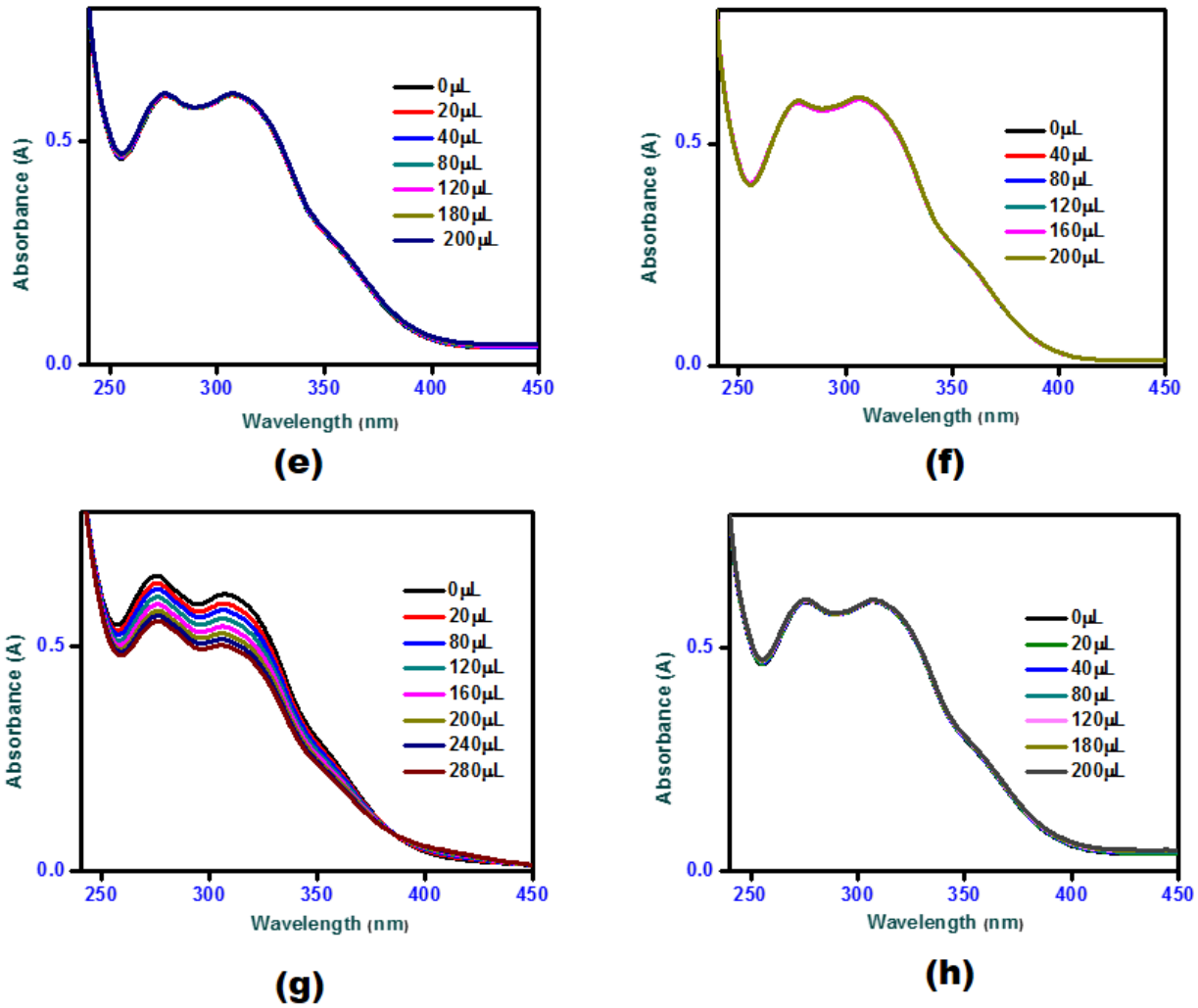

Figure S25: Absorption spectral variation of complex **3** (2 x 10^{-5} mol dm^{-3}) with the addition of 1-5 equivalent of nitrate salts (2 x 10^{-4} mol dm^{-3}) of **(e)** Cr^{3+} **(f)** Mn^{2+} **(g)** Ni^{2+} **(h)** Zn^{2+}in DCM-methanol (1:9).

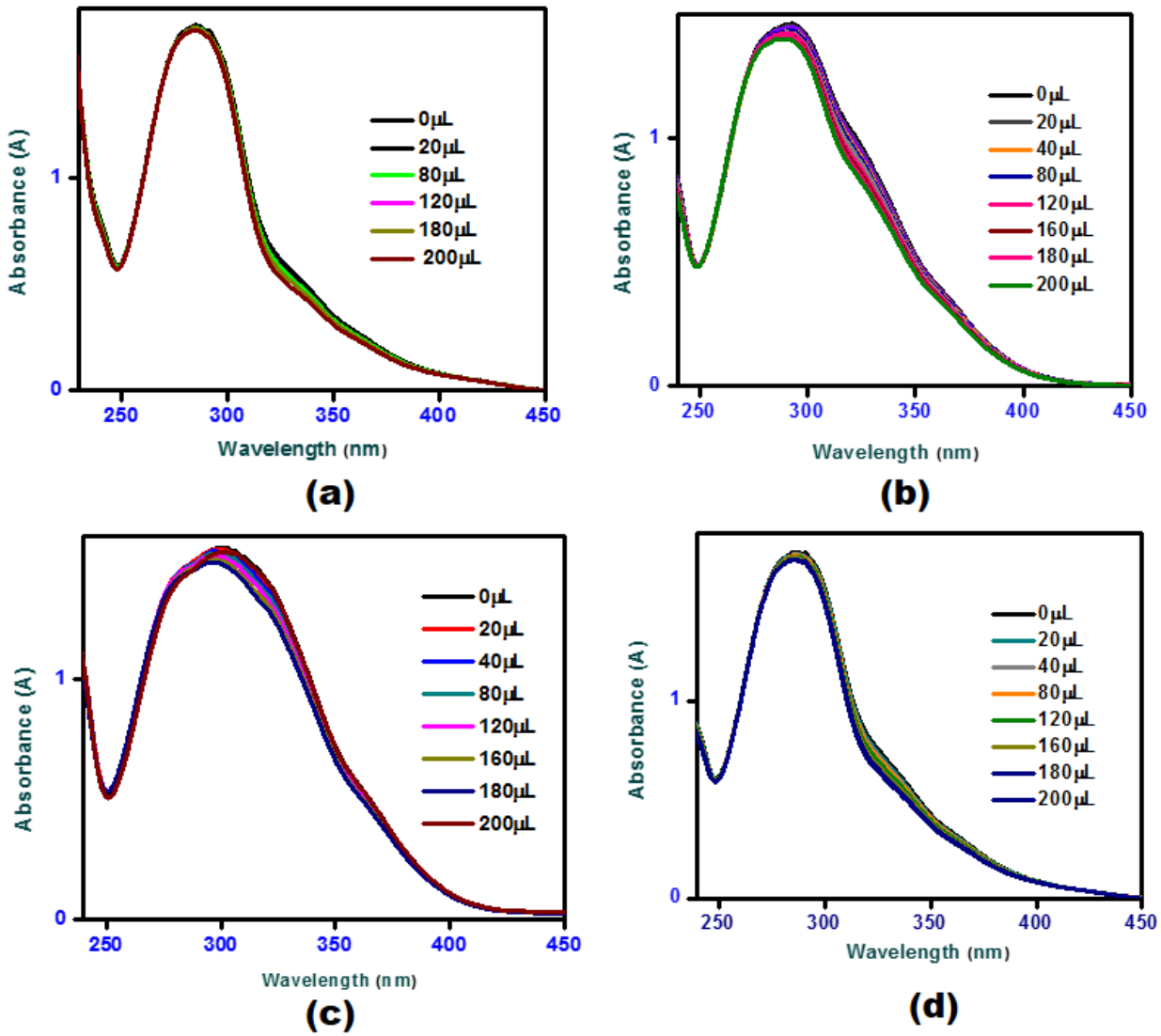

Figure S26: Absorption spectral variation of complex **4** (2 x 10^{-5} mol dm^{-3}) with the addition of 1-5 equivalent of nitrate salts (2 x 10^{-4} mol dm^{-3}) of **(a)** Ag^{+} **(b)** Ba^{2+} **(c)** Cd^{2+} **(d)** Co^{2+}in DCM-methanol (1:9).

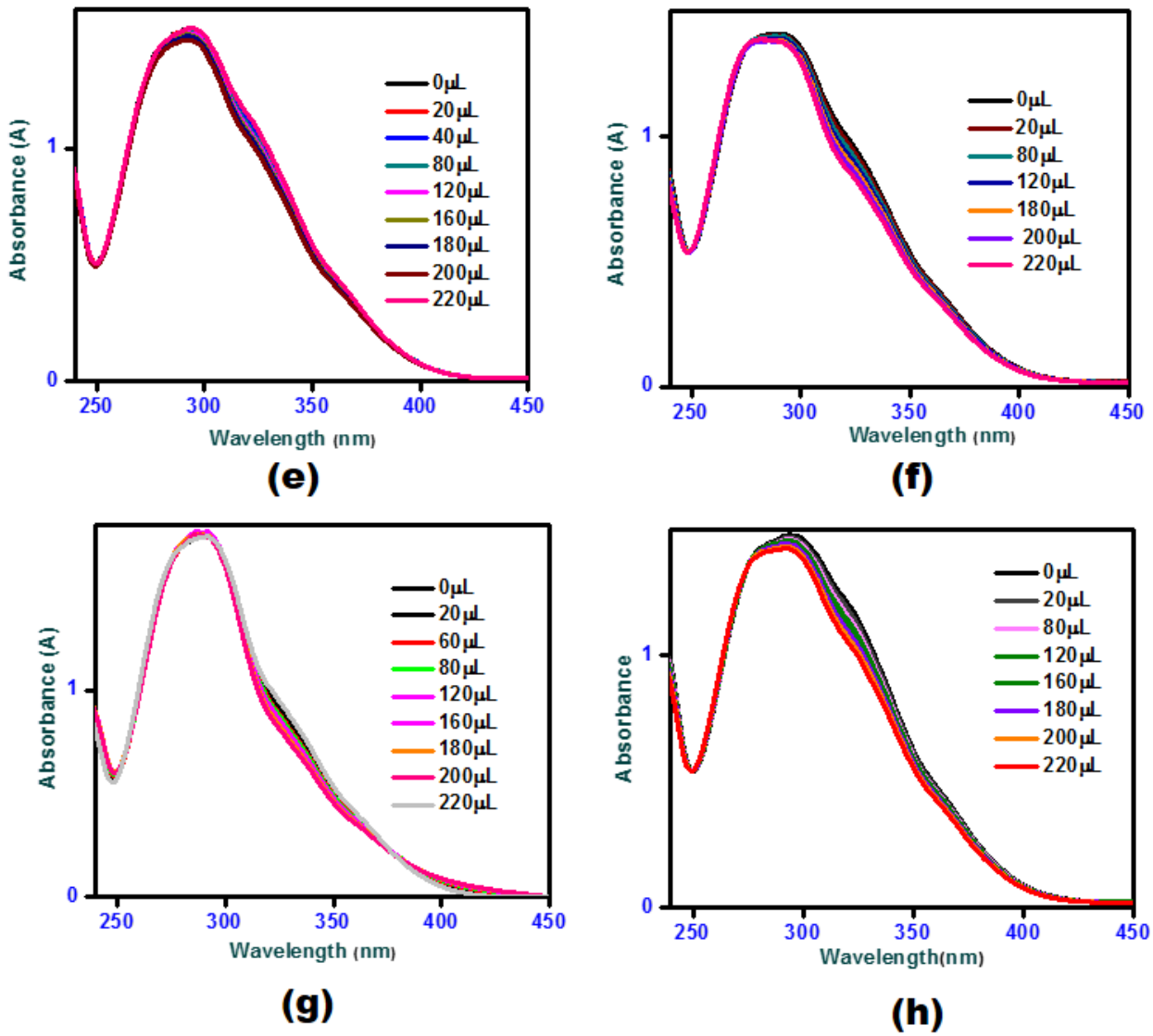

Figure S27: Absorption spectral variation of complex **4** (2 x 10^{-5} mol dm^{-3}) with the addition of 1-5 equivalent of nitrate salts (2 x 10^{-4} mol dm^{-3}) of **(e)** Cr^{3+} **(f)** Mn^{2+} **(g)** Ni^{2+} **(h)** Zn^{2+}in DCM-methanol (1:9).

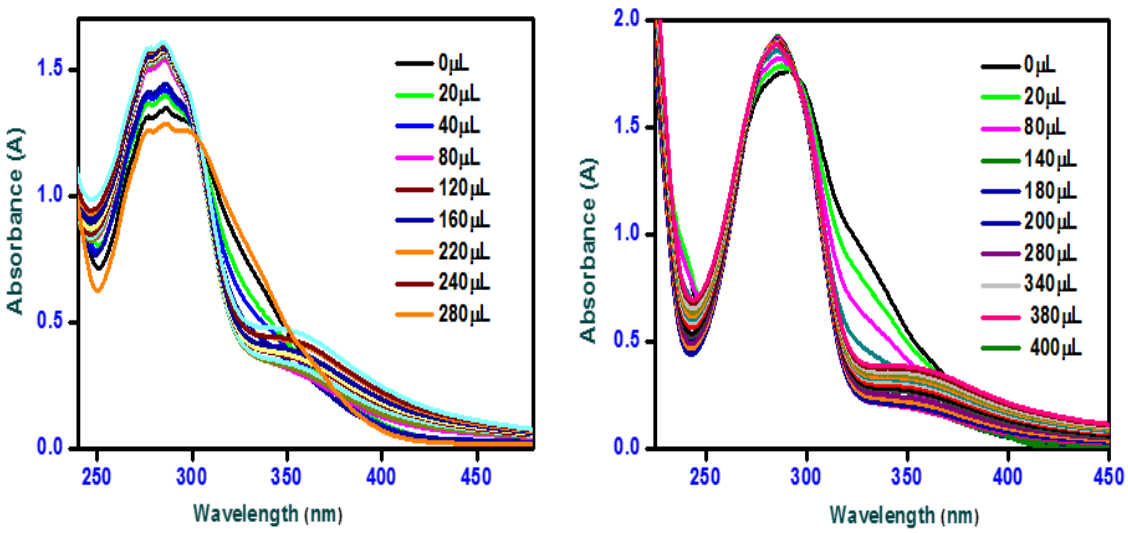

Figure S28: Absorption spectral variation of complex **2** and **4** (2×10^{-5} mol dm^{-3}) with the addition of 1-5 equivalent of ferric nitrate nonahydrate (2×10^{-4} mol dm^{-3}) in DCM-methanol (1:9).

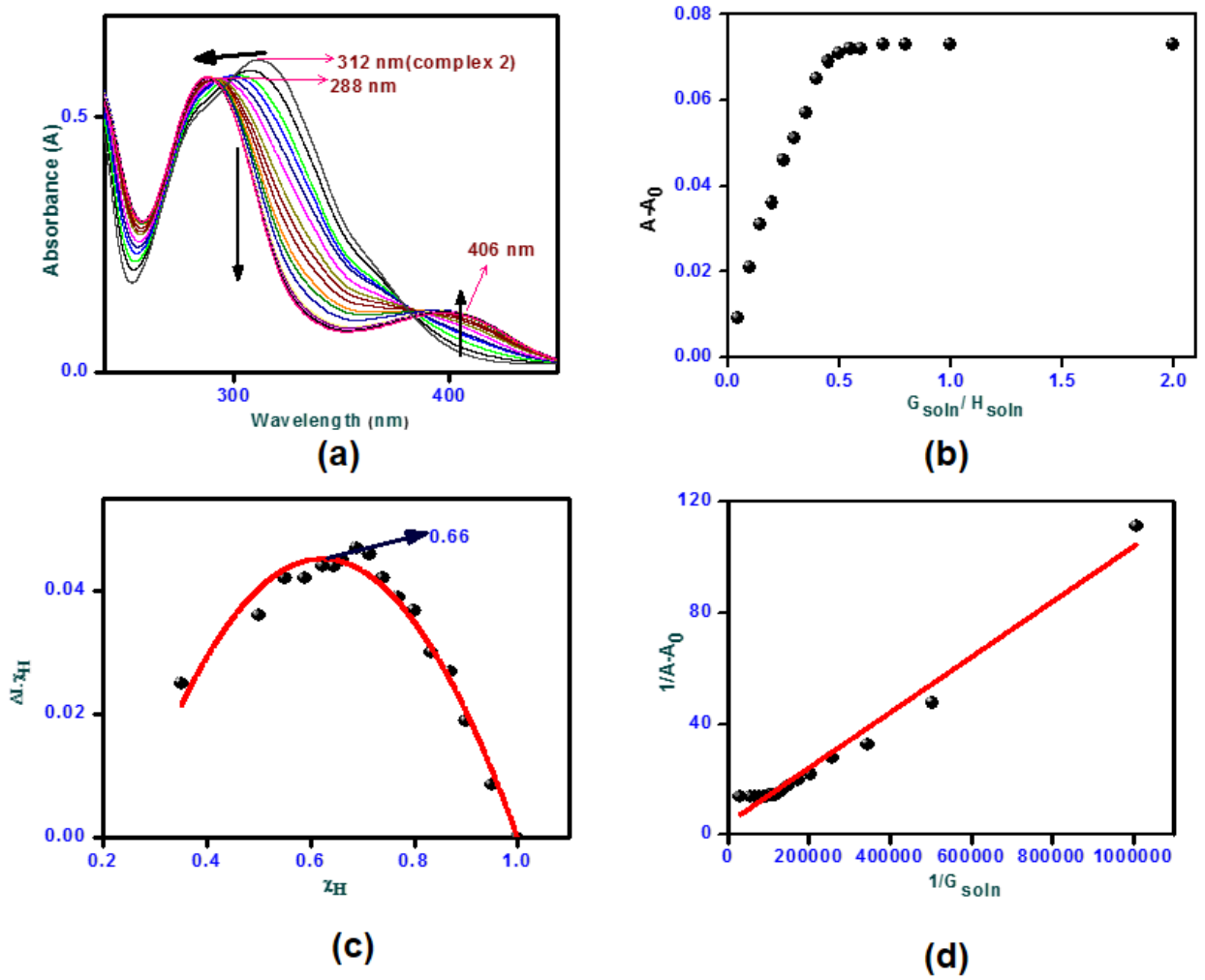

Figure S29: (a) Absorption spectral variation of complex **2** (2 x 10^{-5} mol dm^{-3}) with the addition of 1-5 equivalent of copper(II) nitrate trihydrate (2 x 10^{-4} mol dm^{-3}) in DCM-methanol (1:9). **(b)** The stoichiometric plot of complex **2** with copper(II) nitrate trihydrate. **(c)** Job's plot of Complex **2** with copper(II) nitrate trihydrate. (**d)** Benesi-Hildebrand plot complex **2** with the addition of copper(II) nitrate trihydrate.

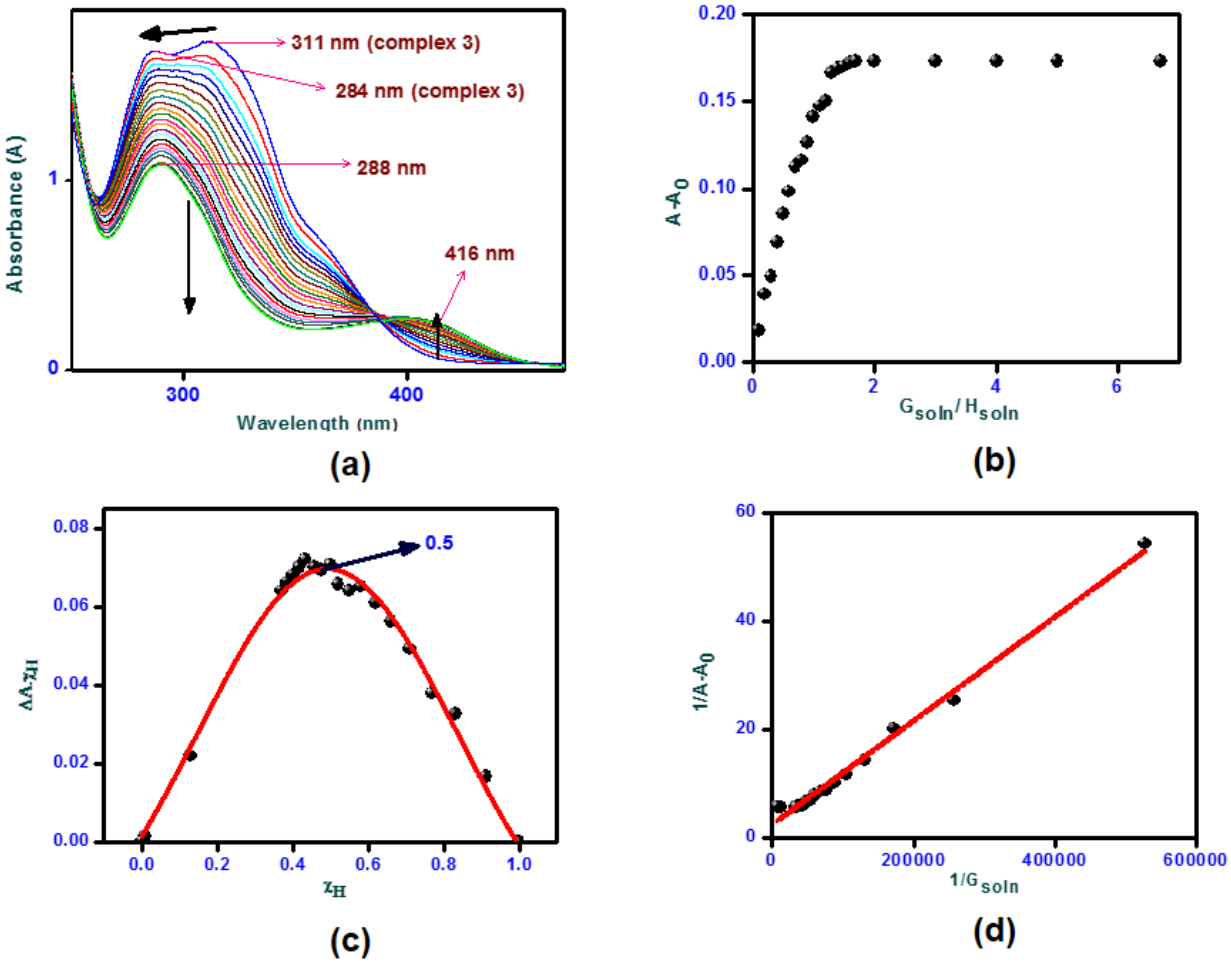

Figure S30: (a) Absorption spectral variation of complex **3** (2 x 10^{-5} mol dm^{-3}) with the addition of 1-5 equivalent of copper nitrate trihydrate (2 x 10^{-4} mol dm^{-3}) in DCM-methanol (1:9). **(b)** The stoichiometric plot of complex **3** with copper(II) nitrate trihydrate. **(c)** Job's plot of Complex **3** with copper(II) nitrate trihydrate. (**d)** Benesi-Hildebrand plot complex **3** with the addition of copper(II) nitrate trihydrate.

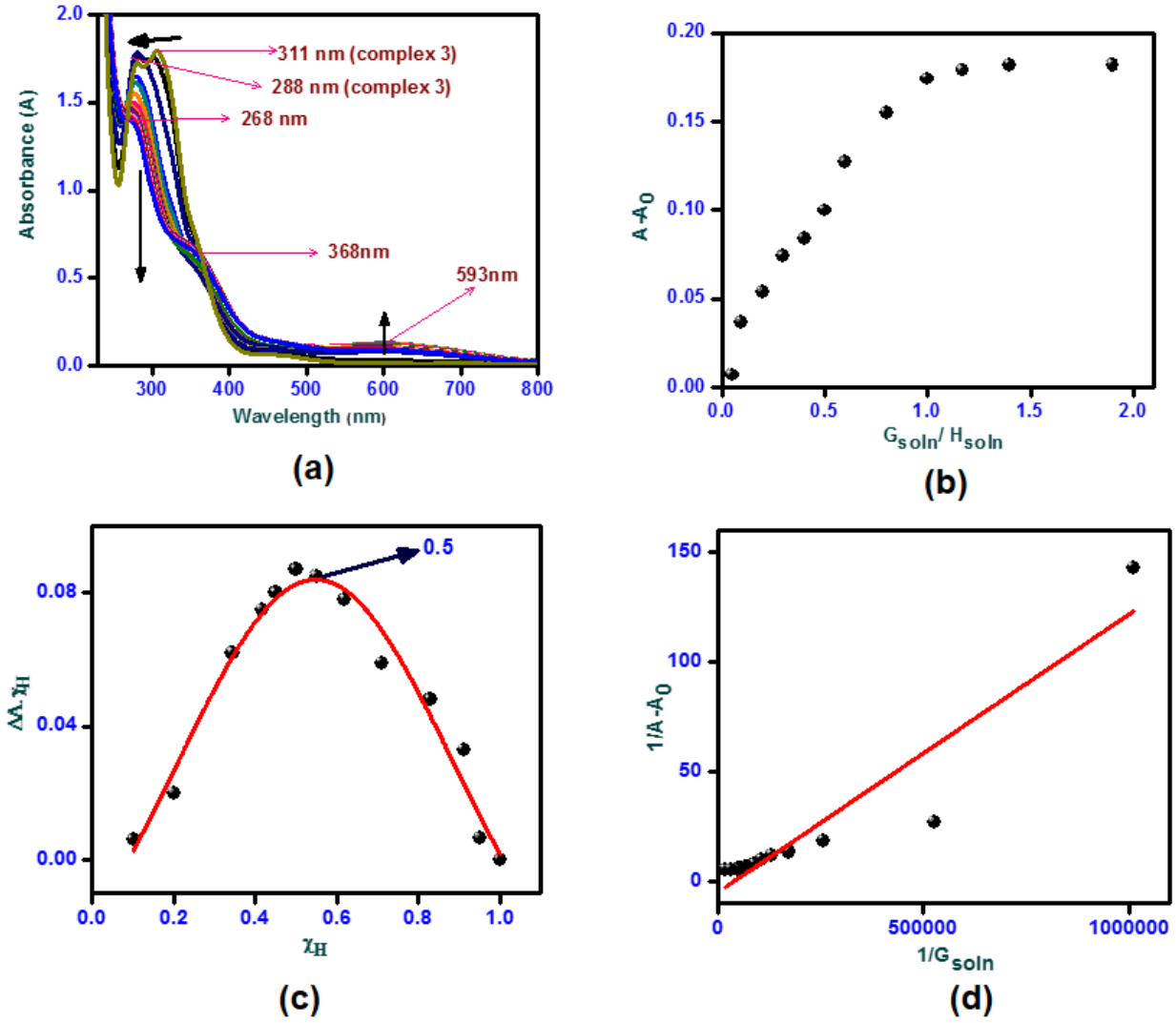

Figure S31: (a) Absorption spectral variation of complex **3** (2 x 10^{-5} mol dm^{-3}) with the addition of 1-3 equivalent of ferric nitrate nonahydrate (2 x 10^{-4} mol dm^{-3}) in DCM-methanol (1:9). **(b)** The stoichiometric plot of Complex **3** with ferric nitrate nonahydrate. **(c)** Job's plot of Complex **3** with ferric nitrate nonahydrate. (**d)** Benesi-Hildebrand plot complex **3** with the addition of ferric nitrate nonahydrate.

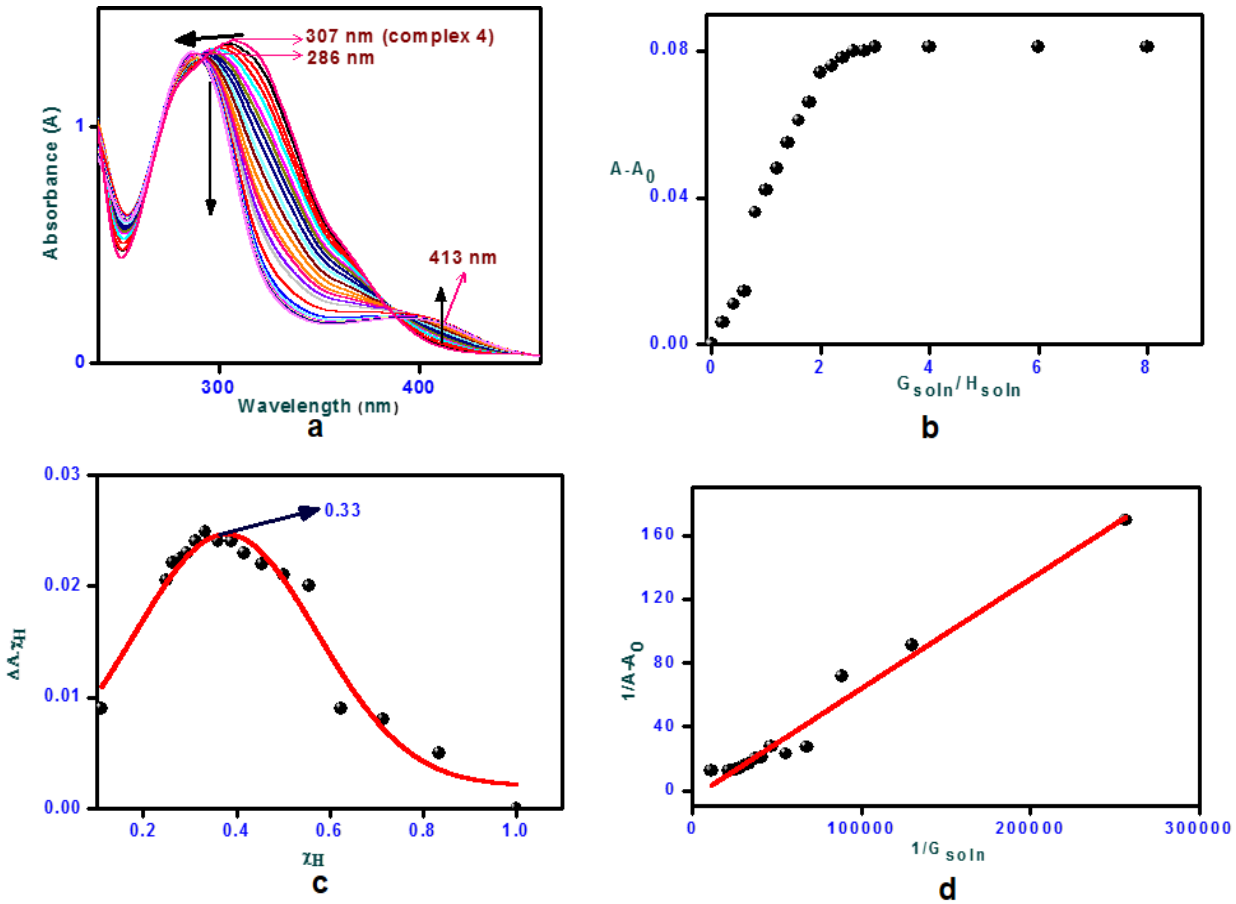

Figure S32: (a) Absorption spectral variation of complex **4** (2 x 10^{-5} mol dm^{-3}) with the addition of 1-5 equivalent of copper nitrate trihydrate (2 x 10^{-4} mol dm^{-3}) in DCM-methanol (1:9). **(b)** The stoichiometric plot of complex **4** with copper(II) nitrate trihydrate. **(c)** Job's plot of complex **4** with copper(II) nitrate trihydrate. (**d)** Benesi-Hildebrand plot complex **4** with the addition of copper(II) nitrate trihydrate.

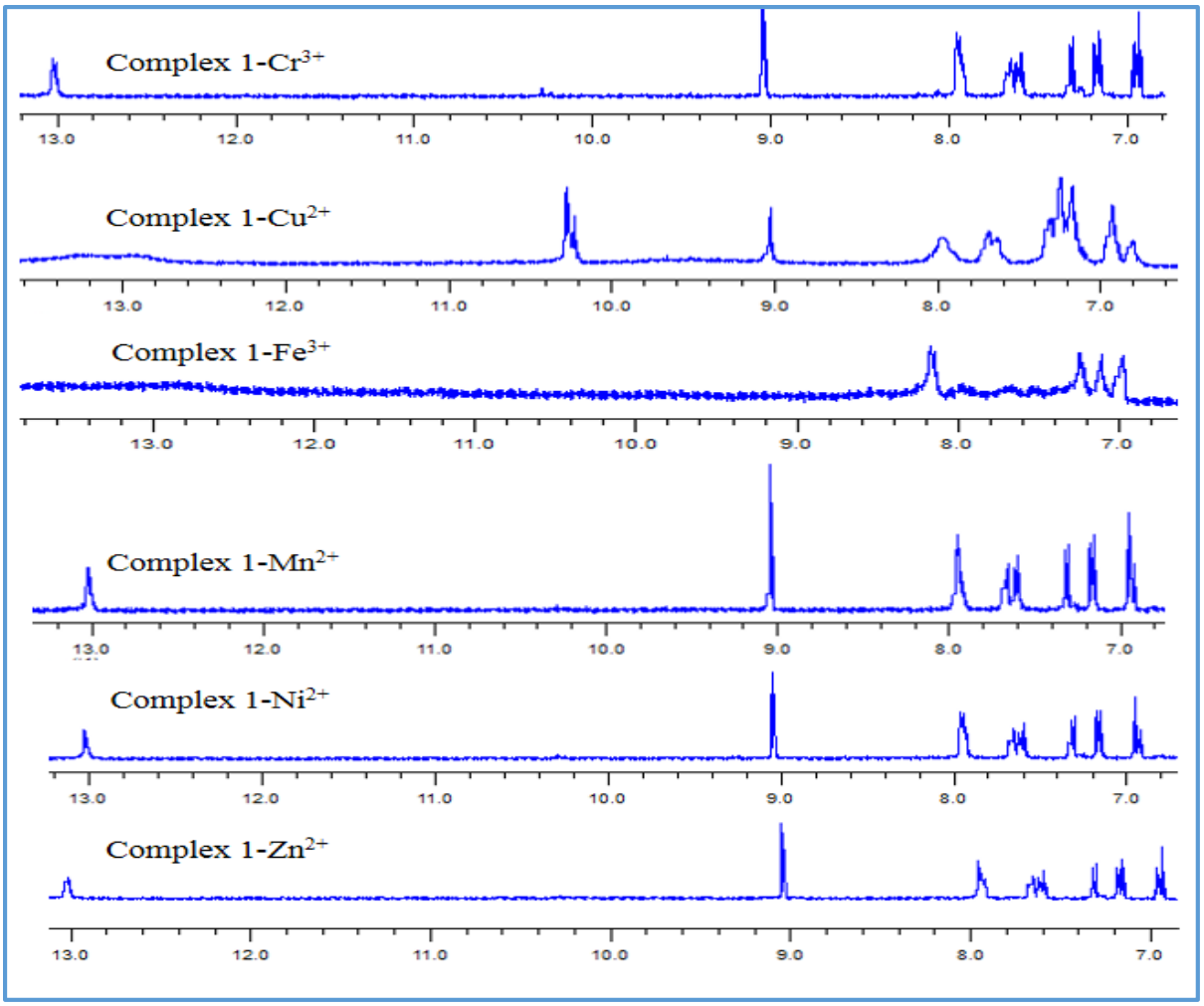
Complex 1-Cr3+
Complex 1-Cu2+
Complex 1-Fe3+
Complex 1-Mn2+
Complex 1-Ni2+
Complex 1-Zn2+
13.0
12.0
11.0
10.0
9.0
8.0
7.0

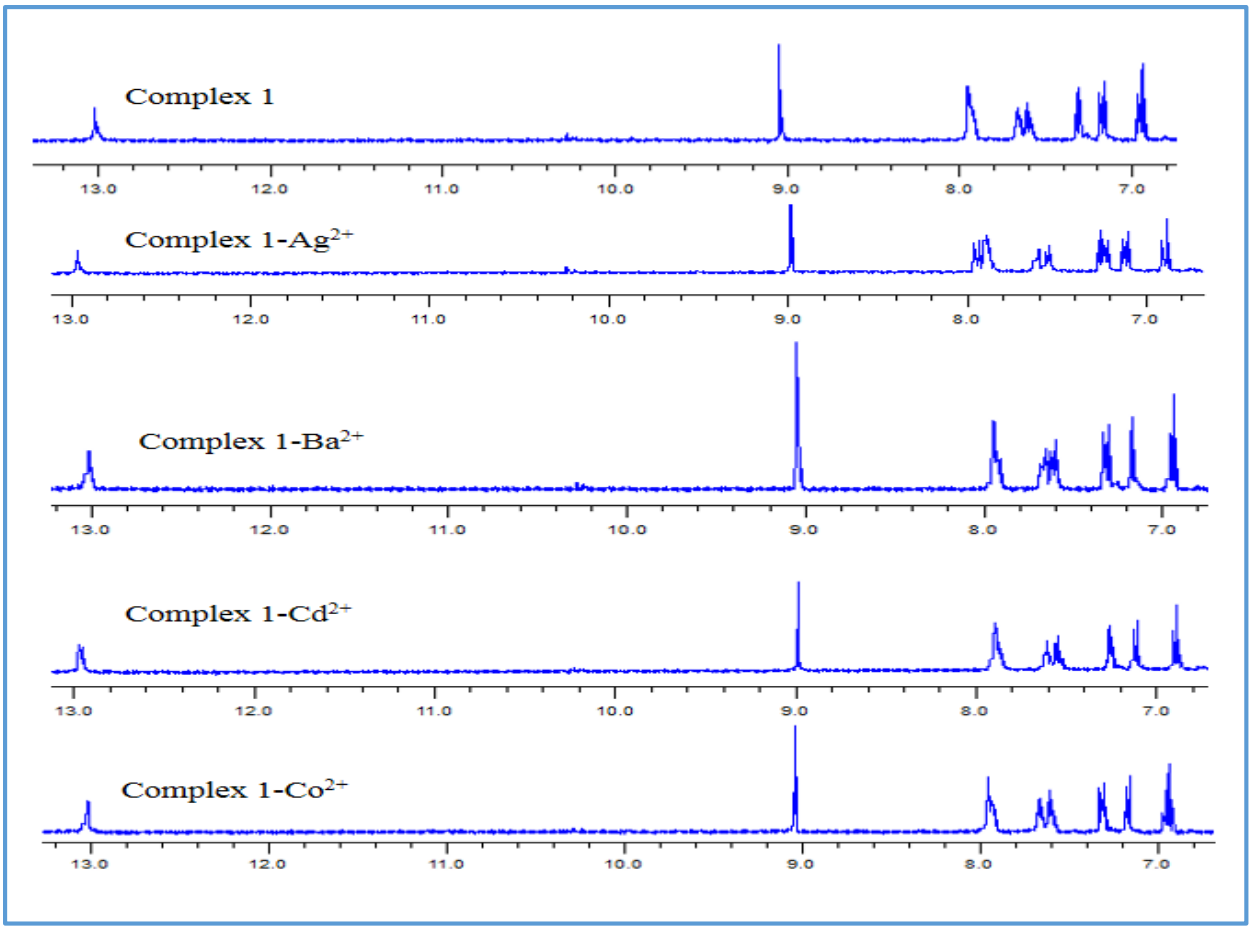

Figure S33: Changes in partial ^{1}H NMR spectra of complex **1** with the addition of an equivalent amount of selected metal ions in DMSO-d_6.

LOD (Limit of Detection) for complex 1-4 with Cu^{2+} and Fe^{3+} ion

LOD was calculated for all complexes with Cu^{2+} and $Fe^{3+}$was calculated on the basis of absorption data. To determine the standard deviation for the absorbance, the absorbance of the individual receptors without any cation was measured by 15 times and the standard deviation of blank measurements was calculated.

The limit of detection (LOD) of the receptors for sensing Cu^{2+} and Fe^{3+} was determined from the following equation:

LOD = K × SD/S

Where K = 3 (according to IUPAC consideration); SD is the standard deviation of the blank receptor (complex **1**-**4**) solution; S is the slope of the calibration curve. From the linear fit graph, we get a slope for all complexes. Thus using the above formula we get the Limit of Detection.

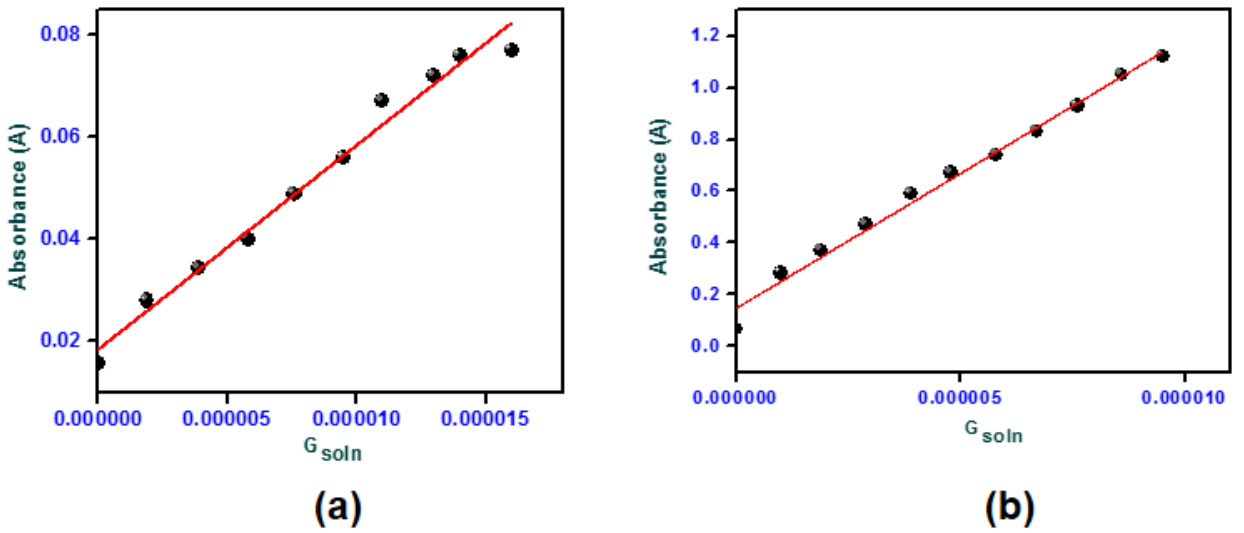

Figure S34: Graph between absorbance and concentration of guest for calculation of slope for **(a)** Cu^{2+} **(b)** Fe^{3+} for complex **1**.

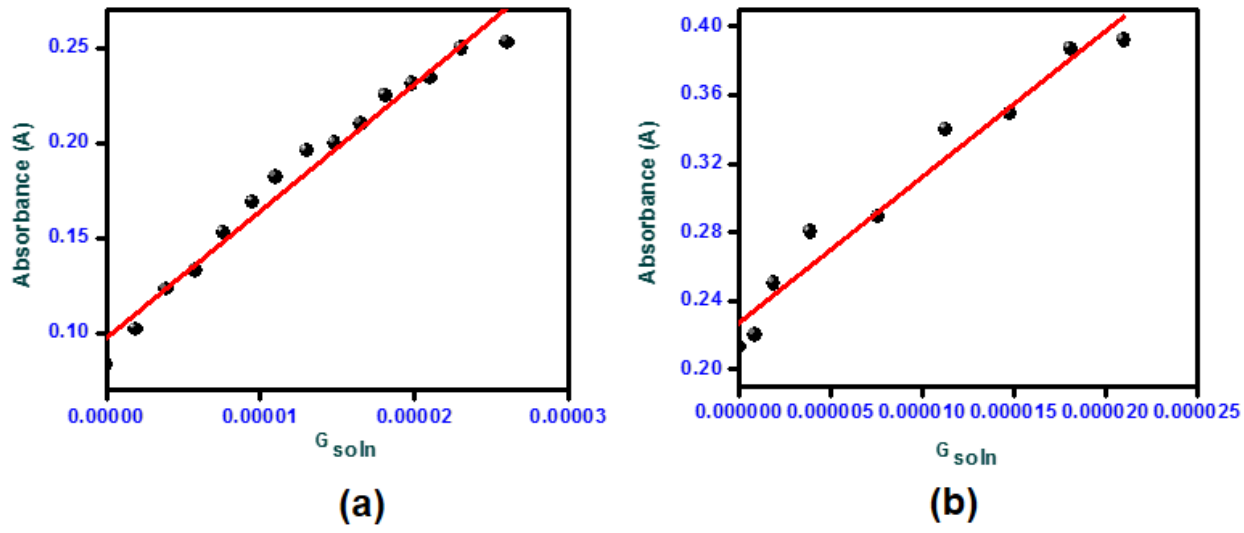

Figure S35: Graph between absorbance and concentration of guest for calculation of slope for **(a)** Cu^{2+} **(b)** Fe^{3+} for complex **3**.

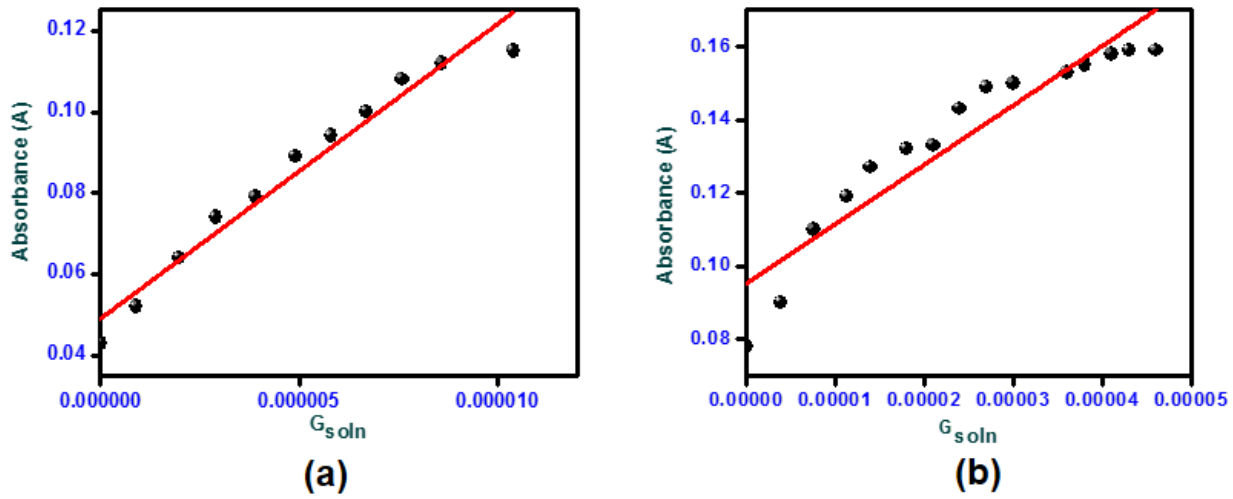

Figure S36: Graph between absorbance and concentration of guest for calculation of slope for **(a)** Cu^{2+} for complex **2 (b)** Cu^{2+} for complex **4**.

X-ray crystallography

The intensity data of **1-4** were collected on a Rigaku SuperNova diffractometer equipped with an Eos S2 CCD detector, using MoKα radiation with graphite monochromator (λ = 0.71073 Å) at T = 293(2) or 100(2) K. The structure was solved by SHELXT and refined on F^2 by full-matrix least-squares methods using SHELXL using Olex2 as the graphical interface.[1-2] Non-hydrogen atoms were anisotropically refined. H-atoms were included in the refinement on calculated positions riding on their carrier atoms. The function minimized F_o^2) from counting statistics. The function R_1 and wR_2 were ($\sigma||F_o|$ - $|F_c||$) / $\sigma|F_o|$ and [σw (F_o^2 - F_c^2)^2 / $\sigma(wF_o^4)$]$^{1/2}$, respectively. Crystallographic data (excluding structure factors) for the structures reported in this paper have been deposited in the Cambridge Crystallographic Data Centre as a supplementary publication no. CCDC 1895986-1895989. Copies of the data can be obtained free of charge on application to CCDC, 12 Union Road, Cambridge CB21EZ, UK (fax: + (44)1223-336-033; email: deposit@ccdc.cam.ac.uk

References:

1. Sheldrick, G.M., Crystal structure refinement with ShelXL, *Acta Cryst.*, (2015), C71, 3-8.

2. O.V. Dolomanov and L.J. Bourhis and R.J. Gildea and J.A.K. Howard and H. Puschmann, Olex2: A complete structure solution, refinement and analysis program, *J. Appl. Cryst.*, (2009), **42**, 339-341.